

# PREDICTIVE MAINTENANCE: THE FEASIBILITY OF A NON-STRAIGHT EDGE KNIFE SHARPNESS DETERIORATION MODEL

---

Master Thesis: Industrial Engineering & Management - Specialization: Advanced Production Engineering

**Author: P. A. Tjabbes**



Date: 12-7-2018

First supervisor: Prof. dr. B. (Bayu) Jayawardhana

Second supervisor: Prof. dr. A. (Antonis) Vakis



university of  
groningen

faculty of science  
and engineering

## ABSTRACT

---

In September 2013 the European Union (EU) announced that the sugar quota system would end in September 2017. As a result the sugar price in the EU declined nearly 50% in five years, forcing sugar production facilities to drastically increase their efficiency. SuikerUnie Ververlaten scaled up its throughput and tried to optimize the sugar to water diffusion through increased cossette (sliced beets) quality. Optimized diffusion requires less water, consequently lowering the energy cost related to evaporation. Determining the optimal knife operation time increases cossette quality. A deep learning algorithm was implemented to decide which slicer should have its knives changed. Due to the nature of an organic product and the available data provided to the model, an accuracy of only 60% was realized.

The aim of this research is to prove the feasibility of a knife sharpness deterioration prediction model through the analysis of non-straight edge factory knives that experienced deterioration under specific input settings while side-lining the effect of external factors. While knowledge of knife sharpness related to cutting soft solids is widely available, no benchmark is mentioned for knives with a non-straight edge blade geometry.

Three knife sharpness measurement methods were customized, applied and verified. It was found that two out of three methods could be successfully implemented for non-straight edge blades. But were not usable as standalone variables due to the accuracy limits required to quantify the input variables at Ververlaten. However, constants acquired from the knife analysis observed at steady state cutting proved that quantifying the input settings is possible and multiple findings lead to further research opportunities to accurately quantify variables.

# TABLE OF CONTENT

---

Abstract	1
List of figures	4
Glossary	6
1 Problem analysis	8
1.1 Problem background	8
1.1.1 The hydraulic balance of sugar production	9
1.1.2 Sugar Production Process at Vierverlaten	9
1.2 Research scope	11
1.3 The system and a Conceptual model	12
1.3.1 System	12
1.3.2 Input, input settings and output	12
1.3.3 External factors	13
1.3.4 Key Performance Indicators	13
1.3.5 Cossette quality and characteristics	14
1.4 Stakeholder Analysis	16
1.5 The research objective	16
1.6 Research questions	17
1.7 Research design and structure	18
2 Theoretical background	19
2.1 General application of knife sharpness	19
2.2 Sharpness determined through optical and mechanical techniques	20
2.3 Non-straight edge knife sharpness	21
2.4 Measurement techniques	22
2.4.1 Indentation parameter	22
2.4.2 Blade Sharpness Index parameter	22
2.4.3 Cut initiation parameter	23
3 Verification of knife sharpness methods	24
3.1 Indentation method	24
3.2 BSI method	26
3.2.1 First test run and data processing	27
3.2.1.1 Substrate type verification	28
3.2.2 Second test run: Speed and substrate width	29
3.2.2.1 Indentation speed verification	29
3.2.2.2 Substrate width verification	29
3.2.3 Third test run: Comparing knives	30

3.2.3.1	Number of test required per knife for sharp and blunt knives.	30
3.2.4	Fourth test run: Polymer substrate	32
3.3	Applied research setup	32
3.4	Knife collection	33
3.4.1	Elimination of external factors	33
4	Results	34
4.1	Fracture toughness and the BSI	34
4.2	Blunt knife analysis	35
4.3	Factory sharpened knives compared	36
4.4	Quantifying knife sharpness variables	37
4.4.1	Difference cutting speed over 40cm blade (60%)	38
4.4.2	Location under Beet bunker	39
4.4.3	Different revolutions per minute	40
4.5	Research questions	41
5	Discussion and conclusion	42
5.1	Result discussion	42
5.2	The limitations	44
5.3	Conclusion	44
	References	46
	Appendix A: Beet production	48
A1	Beets & transport	48
A2	Reception	48
A3	Washing	48
A4	Slicing of the beet	48
A5	Juice production	50
A6	Purification of the juice	51
A7	Juice concentration	52
A8	Crystallization and centrifugation	52
	Appendix B	53
B1	Layout of the slicers underneath the beet bunker.	53
B2	Schematic and detailed layout of the juice production	54

## LIST OF FIGURES

Figure 1: The European and world market sugar price. A decline in price difference after the 2013 announcement to end the EU sugar quota can be observed. (EU Sugar Market Observatory)	8
Figure 2: The process steps for Sugar Production from sugar beets at SuikerUnie Ververlaten.	10
Figure 3: Left) Sample of cossette, Right) A new knife that is used at Ververlaten to produce cossettes, and the Fraiser that is used in a grinding machine to sharpen the knives.	11
Figure 4: Conceptual model of the slicer - Focus of paragraph 1.3	12
Figure 5: A cutting disk is placed horizontally in a slicer. Each cutting disk contains 24 knife blocks. Knife blocks can be removed from the slicer to change the two 20cm wide knives with sharp knives.	13
Figure 6: The A and B knives have a triangular wave pattern. The wave pattern of B-knives are shifted half a period with respect to the wave pattern of A-knives. Knife blocks containing either A-knives or B-knives are placed in alternating order to create V shaped cossettes in four consecutive cuts.	15
Figure 7: Cross-sectional view of the different cossette geometries produced by a slicer. From left to right: Type-1, Type-2, Type-3 and Type-4. Type-1 is ideal but in reality non-existent. The type-3 and type-4 are produced at Ververlaten.	15
Figure 8: The empirical cycle as proposed by Wieringa to conduct knowledge based research. (Wieringa, 2014)	18
Figure 9: (left an example of a finite element analysis model containing the forces around the tip. Right) Optical image analysis (McCarthy et al., 2010) .	20
Figure 10: (Left) Image of an A and B knife used at Ververlaten. Type-A and type-B knives alternate each other to create Type-4 V shaped cossettes. (Right) A close-up of a new knife at the bottom and a sharpened used knife on top, where it is clearly visible that the surface roughness of the used knife highly increases after 9.1 mm of indentation.	21
Figure 11: Cross sectional schematic image of a straight edge knife during different stages in the cutting process. (a) Cut initiation moment, (b) Just after cut initiation the substrate material travels up the side of the blade, (c) the moment at which the material re-joins and the whole knife travels through the substrate, (d) Steady state cutting through a material	22
Figure 12: Schematic image of the concept setup to verify the indentation parameter. An arm (1) is connected to a hinge (2) with the knife (4) attached at the other end. A movable weight (3) is used to control the potential energy at user specified drop heights. The indentation into the substrate (5) measured in mm is the parameter indicating the sharpness of a knife.	24
Figure 13: The results of the concept cutting test including the average (avg.) indentation.	25
Figure 14: Photograph of the machine (MTS810) used for the cutting trials	26
Figure 15: Raw graph from the data the MTS810 machine produces. The method described in section 3.2.1 transforms the data of each test to usable data as can be seen in Figure 17.	27
Figure 16: Distribution of the stiffness while the knife is traveling towards the substrate.	28
Figure 17: Data graphs from the first cut test. A new factory knife (Figure 10) is used to cut through a horizontally placed $60 \times 10 \times 10 \text{ mm}^3$ potato substrate with 0.5 mm/s. (A) The point of contact between the knife and the substrate. (B) The point at which cutting initiates. (C) The point at which normal cutting continues (D) The point at which the second wedge angle enters the substrate. (E) Steady cutting through the substrate. (F) Continues steady state cutting.	28
Figure 18: Graph containing six cut tests. A new factory knife (Figure 10) is used to cut through horizontally placed potato substrates with 0.5 mm/s. The highest two graphs cut through a $60 \times 10 \times 10 \text{ mm}^3$ substrate, the middle two graphs cut through a $40 \times 10 \times 10 \text{ mm}^3$ , and the lower two graphs cut through a $10 \times 10 \times 10 \text{ mm}^3$ substrate.	30
Figure 19: A blunt and a mildly blunt knife are tested 2 and 4 times.	31
Figure 20: Five cut tests are performed with a new sharp knife. Results should be similar but they are not because test results from manually preparation of substrates are not objective.	31

Figure 21: A new sharp knife is used to cut through horizontally placed substrates with 0.25 mm/s. The first tests with the polymer show that the required data contains the points required to calculate the BSI. Repetition of the test show similar results.	32
Figure 22: The left graph contains the cutting force of, P the first pass through a polymer substrate, X the free pass through the same substrate, and X-P the net graph that displays the cutting force without friction. The right graph contains the results corrected for the knife surface area A from Eq.2	34
Figure 23: The BSI of a sharp factory knife measured multiple times for different substrates and substrate widths.	35
Figure 24: Parameter comparison for a blunt and a sharp knife.	35
Figure 25: The polymer cutting force of a sharp and a blunt knife compared.	36
Figure 26: Comparing cutting test parameter of a new knife, a knife sharpened after fraiser replacement and a knife sharpened before fraiser replacement	36
Figure 27: Cutting test performed on knives collected after 0, 3, 6, 11, 16 and 24 hours. Values for three parameters at $x = 8.0mm$ plotted against the hours of production.	38
Figure 28: Comparing knife sharpness at different distances from the rotating axle.	39
Figure 29: Comparing knives from four slicers in a row after 20 hour simultaneous production.	39
Figure 30: Comparing knives from two slicers that produced at 27 and 37 RPM. Right: the stiffness graph of a questionable sample.	40
Figure 31: The left knife is sharpened at the factory and has a clear frontal angle. The right knife is new and has no frontal angle.	42
Figure 32: Cross-sectional side and top view drawing of a beet slicer at Viervelaten. The red parts indicate the location of the sugar beets during operation. Washed beets enter the slicer at the top and flow towards the top surface of the cutting disk. The cutting disk changes the beets into cossettes.	49
Figure 33: A flow diagram of the control system which ensures a predetermined target capacity is maintained.	50
Figure 34: Cross-sectional side view drawing of a knife used at Viervelaten installed in a knife block.	50
Figure 35: Graph displaying the breakdown of Pectin for increased temperature and/or increased pH. This negatively influence the strength of the cossettes. Dutch translation (van der Poel, Schiweck, & Schwartz, 1998b)	51
Figure 36: A top view of the slicer layout underneath the beet bunker. Each row is connected to a different brewing trough (BT). Slicer 10 can either be connected to BT1 or BT3. Furthermore, the row from slicer 15 is connected to BT4 and the row from slicer 14 is connected to BT1. Each BT is connected to a Diffusion tower. So TB4 is connected to diffusion tower 4. However, due to incremental factory expansions and flexibility an extra diffusion tower (DT3) is used. DT3 is connected to BT4 and BT1. The bottom row of slicers is only connected to BT1 and DT1.	53
Figure 37: Schematic cross section of the juice production step. Cossettes enter the brewing through at the top left for mixing and heating to 70 degrees C. The mixture is pumped to the bottom of the diffusion. Water enters at the top and the counter current flows ensure optimal diffusion. The mixture leaves the diffusion tower at the bottom and enters the brewing through at the top. Thin juice is extracted at the left bottom of the brewing through.	54

## GLOSSARY

---

Name	Meaning
Backend factory	The production steps at Vierverlaten after juice purification
Beet bunker	The temporary storage above the slicers containing washed beets
Beet campaign	Beet-processing season: The period during which beets are harvested and the factory processes them
Brix	Refractometric dry substance called Brix: The dry-substance content measured by refractometer expressed as mass percentage
Colloids	High molecular substances such as pectin, dextran, colouring materials, decaying beet particles, and microorganisms found during sugar beet processing
Cossettes	Beet slices produced by a beet slicer
Diffuser	Large, agitated tank in which cossettes slowly move from one end to the other and hot water moves in the opposite direction to diffuse sugar from the cossettes
Dry pulp	The pulp after it is dried in pulp dryers, containing about 10% moisture
Finite element method	(FEM) A numerical method for solving problems for engineering and mathematical physics.
Frontend factory	The production steps at Vierverlaten before juice purification
Hydraulic balance	The relation between the level of water consumption and level of sugar extraction is called the hydraulic balance
Key Performance indicator	(KPI) The KPI indicate the performance measurements of the system
Knife block	A metal box containing two knives. The knife blocks are placed in a cutting disk during production
Multi effect evaporation	In a multiple-effect evaporator, water is boiled in a sequence of vessels, each held at a lower pressure than the last. Because the boiling temperature of water decreases as pressure decreases, the vapour boiled off in one vessel can be used to heat the next, and only the first vessel (at the highest pressure) requires an external source of heat
Musculoskeletal disorders in distal upper extremities	(MSDUE) Disease related to repetition of manual tasks
Mush	Cossettes that are smaller than 1 centimetre
Mush content	(MC) is the ratio of the mass of cossettes less than 10 mm long to the total cossette mass (100 g).

Polarimetric sucrose	The sucrose content measured by polarimetry expressed as mass percentage
Polarization	(Pol) Term used in sugar technology with the same meaning as % polarimetric sucrose
Press water	The juice squeezed from the wet pulp in a pulp press and returned to the diffuser
Pressed pulp	The pulp after pressing (it contains about 70% moisture)
Pulp	Sugar beet fibrous and sugar-depleted material after being separated from the juice in the diffuser
Purity	A sugar term used to describe the percentage (by mass) of sucrose in the total dry substance
Raw sugar	Unrefined sugar consisting of crystals covered with a thin layer of low-purity syrup (in a beet-sugar factory, the crystalline sugars produced in the second and third stages of the crystallization process are called raw sugars)
Silin number	(SN) The length (in meter) of 100 gram cosettes. Acquiring the SN number requires to lay out the random sample of 100 grams lengthwise
Swedish number	(SWN) A ratio formed by the weight of cosettes longer than five centimetre divided by the weight of mush from the same sample.
Tare	Clay, sand, stone, and trash mixed with the beets
Thick juicy	The product of the evaporation station that is fed to the crystallization station
Thin juice	The product of the purification station that is fed to the evaporation station
Wet pulp	The pulp coming from a diffuser, containing about 90% moisture



# 1 PROBLEM ANALYSIS

The problem background is discussed in section 1.1. The slicer is identified as the scope of this research. The conceptual model (section 1.3.1) analyses the system within the scope and concludes with the research objective in section 1.3.5. The chapter concludes with the research design and structure that explains how the research goal and research questions are reached and answered.

## 1.1 PROBLEM BACKGROUND

In 1968 the quota system and support prices for sugar were introduced to help the Common Agricultural Policy (CAP) in Europe to achieve one of its initial goals, namely to improve food self-sufficiency. This was achieved through protection from imports due to the duties and taxes.

In 2014 90% of the EU sugar production was controlled by seven dominant alliances: Sudzucker, Nordzucker, Tereos, ABF (Associated British Foods), Pfeifer and Langen, Royal Cosun and Cristal Union. Cosun took 7<sup>th</sup> place with 7% of the total EU production volume. These companies/alliances controlled nearly 90 % of the total EU sugar quota production. This is also described as an oligopoly by rule of the Herfindahl–Hirschman Index resulting in high sugar prices in the EU (Maitah, Řezbová, Smutka, & Tomšík, 2016). In 2013, the EU countries and the European Parliament agreed to end the sugar import quota system at the end of the 2016/2017 marketing year. Figure 1 displays a price graph for white sugar from 2006 until 2018 in the European Union.

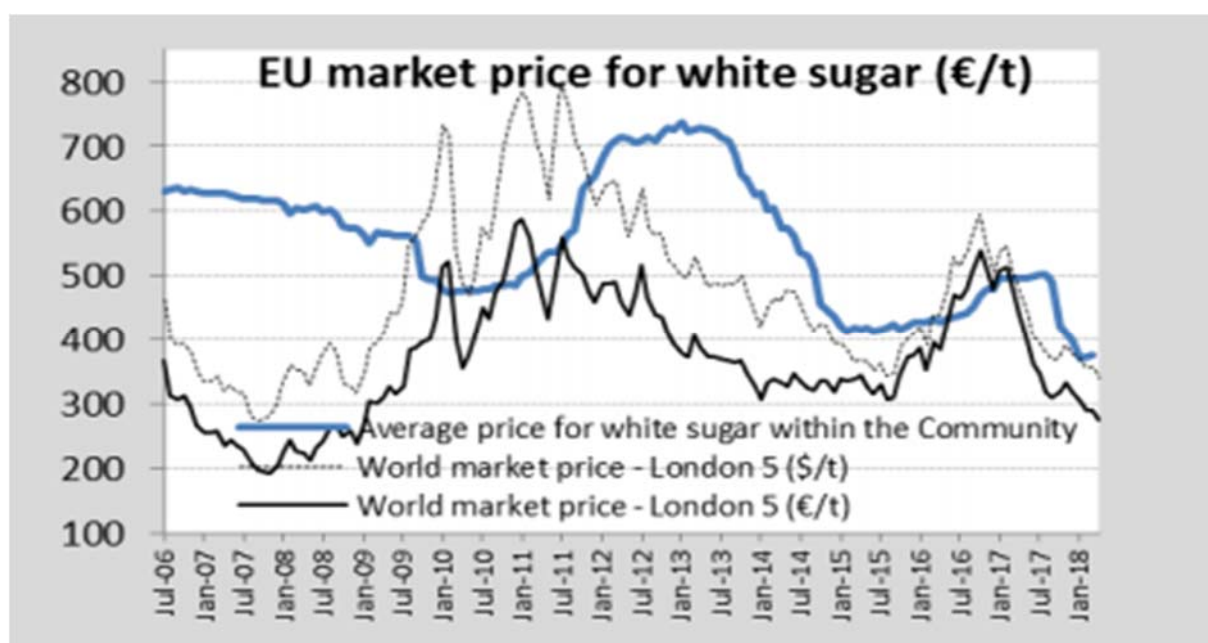


Figure 1: The European and world market sugar price. A decline in price difference after the 2013 announcement to end the EU sugar quota can be observed. (EU Sugar Market Observatory)

Although the global demand for sugar grows 1% annually according to the EU Sugar Market Observatory, the end of the EU sugar quota and the low global sugar price (Figure 1) caused the price for white sugar in Europe to drop. With a lower EU sugar price, the turnover of the aforementioned alliances will drop. This forces European sugar production facilities to be more efficient, SuikerUnie Viervervaten being no exception.

SuikerUnie Ververlaten is located in Hoogkerk, in the province of Groningen, The Netherlands. It is one of three sugar production facilities of the agro-industrial group Royal Cosun. Cosun is a cooperation owned by 8800 shareholders of which mostly farmers. It has an annual turnover of two billion and 3900 employees. Other subsidiaries of Cosun are Aviko, Duynie, Sensus, SVZ and Cosun Biobased Products. They produce ingredients and products that make their way to the food industry, foodservice sector and retail channels.

Cosun houses the Research and Development (R&D) department that focuses on industry wide optimization such as: crop and soil improvements and minimizing transport costs by experimenting with local production. Factory production and process optimizations at Ververlaten are initiated and performed by Ververlaten employees. Minor optimizations are performed throughout the beet campaign and major expansions and machine optimizations are performed after the beet campaign. The beet campaign refers to the harvest and processing of sugar beets.

### **1.1.1 The hydraulic balance of sugar production**

The total sugar content of a sugar beet varies from 10 to 20 percent. Four steps are required to produce sugar from sugar beets. First the beets are sliced, the second step is to transfer the sugar from the beet into water using diffusion. The third step is to boil the sugar water until it becomes thick syrup. The fourth and final step is to cool the thick syrup in order for the sugar to crystallize.

Cost efficient sugar production requires economies of scale. Sugar is the main product produced at Ververlaten. Side products are: animal food, biogas and semi-finished products. The goal is to maximize the extraction of sugar from sugar beets while simultaneously maximizing the output of sugar. After 120 minutes of diffusion roughly 80% of the sugar is extracted from the beet. It requires five times more time and more water to extract 90% of the sugar from the beet. The relation between the level of water consumption and the level of sugar extraction from the beet is called the hydraulic balance. At Ververlaten roughly 70% of the total expenses are energy costs of which the biggest expense is directly related to the evaporation of water. High sugar prices allow higher water consumption and thus better sugar extraction, while lower sugar prices result in lower water usage and lower sugar extraction. Furthermore, after water is used to clean the sugar beets and the factory itself, it can contain up to 0.6% sugar. Appendix A explains how water management at Ververlaten extracts sugar from the washing water.

### **1.1.2 Sugar Production Process at Ververlaten**

Sugar beets are planted around March/April and harvesting starts in September. The beet campaign at Ververlaten starts at first harvest and continues 24 hours, 7 days a week for approximately 150 days. A day is divided into three shifts of 8 hours which are filled by five different teams working according to a schedule.

Full grown sugar beets however, cannot be harvested 150 days per year. Early beets are not fully developed and late beets have to be stored with the risk of freezing. Farmers receive a compensation for early harvest and late harvest. The higher compensation at the start and end of the production period causes prolonged production to become less economically viable.

Figure 2 shows the main production process steps at Ververlaten. The required efficiency improvement as mentioned in the section 1.1 concerns the first frontend factory. The production plant is divided into two parts. The frontend which includes the production steps up until centrifugation and evaporation, and the backend which includes all consecutive steps. In recent

years the capacity of the backed factory was the bottleneck since the crystallizer could not match the throughput of the frontend factory. Building another crystallizer to increase the capacity of the bottleneck costs 40 million euro. A cheaper option was implemented and a storage for thick juice was built in between the frontend and the backend factory. During a beet campaign the frontend and the backend factory operate at full capacity. A small campaign is initiated after the beet campaign when the crystallizers are empty again and only the backend factory is activated to process the stored thick juice.

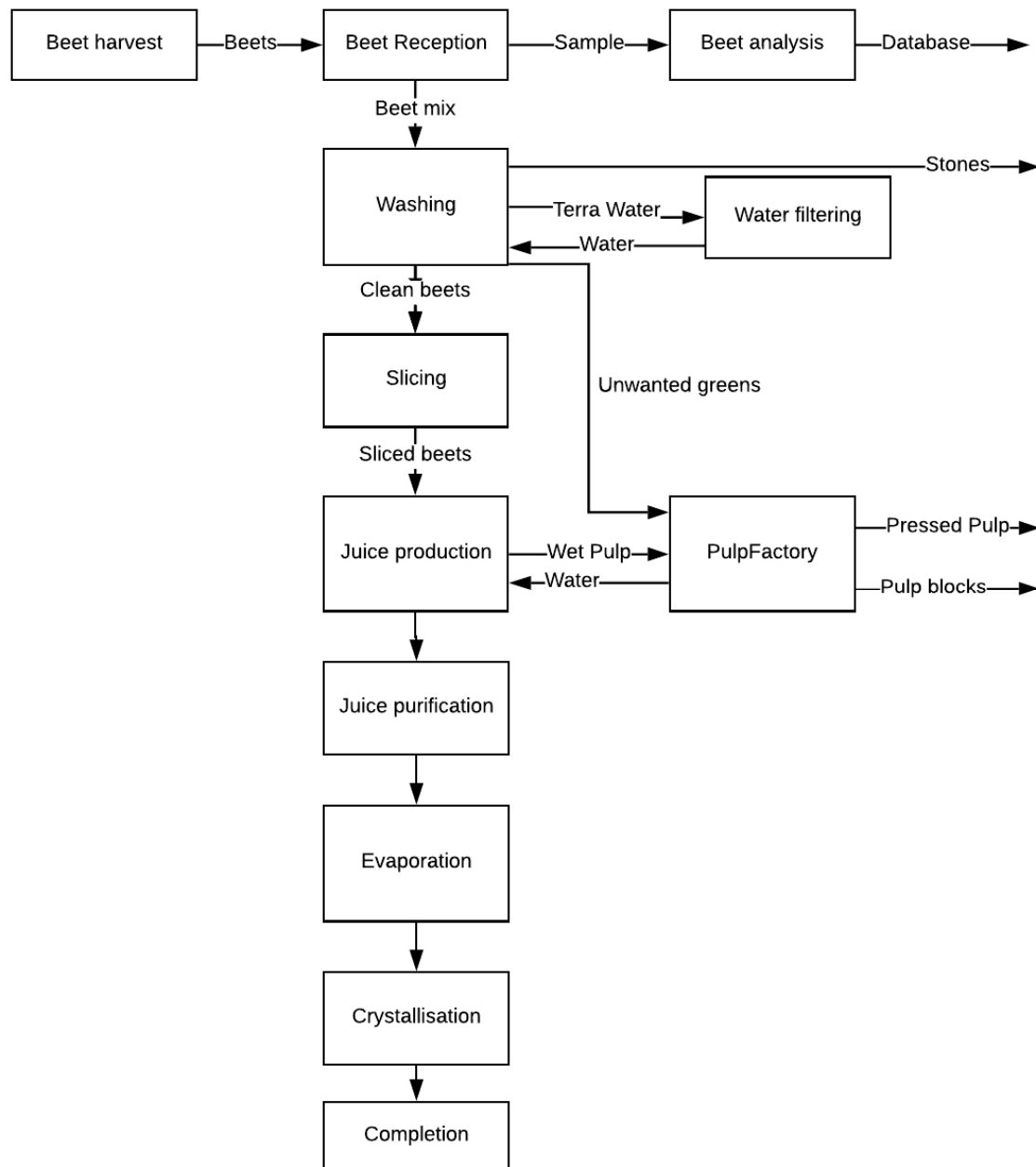


Figure 2: The process steps for Sugar Production from sugar beets at SuikerUnie Ververlaten.

Several sections in this research require knowledge on the production steps at Ververlaten. Appendix A provides detailed information on each production step (Figure 2) and is used throughout this research for referencing.

## 1.2 RESEARCH SCOPE

As explained in Appendix A5 the production process after the juice production stage at Ververlaten has recently been upgraded. The main goal of the frontend factory is optimize sugar extraction from the beet and at the same time minimizing energy and water usage. Water usage will be minimized if the diffusion is optimized through higher quality cossettes. Since cossettes are produced by the slicer the scope of the thesis is restricted to the slicer. An example of cossettes can be found in Figure 3. Cossettes are produced by a slicer with a rotating cutting disk containing 48 knives (Figure 3). Section 1.3 contains an analysis of the slicer system. A conceptual model is made to get a better understanding of the inputs, outputs, external factors and key performance indicators (KPI).



*Figure 3: Left) Sample of cossette, Right) A new knife that is used at Ververlaten to produce cossettes, and the Fraiser that is used in a grinding machine to sharpen the knives.*

## 1.3 THE SYSTEM AND A CONCEPTUAL MODEL

### 1.3.1 System

Figure 4 gives an overview of the system. The main function of the system is to produce high quality cossettes. Quality refers to the ability of cossettes to cost efficiently diffuse sugar into water. The input is affected by the external factors and corrected by a combination of the input settings.

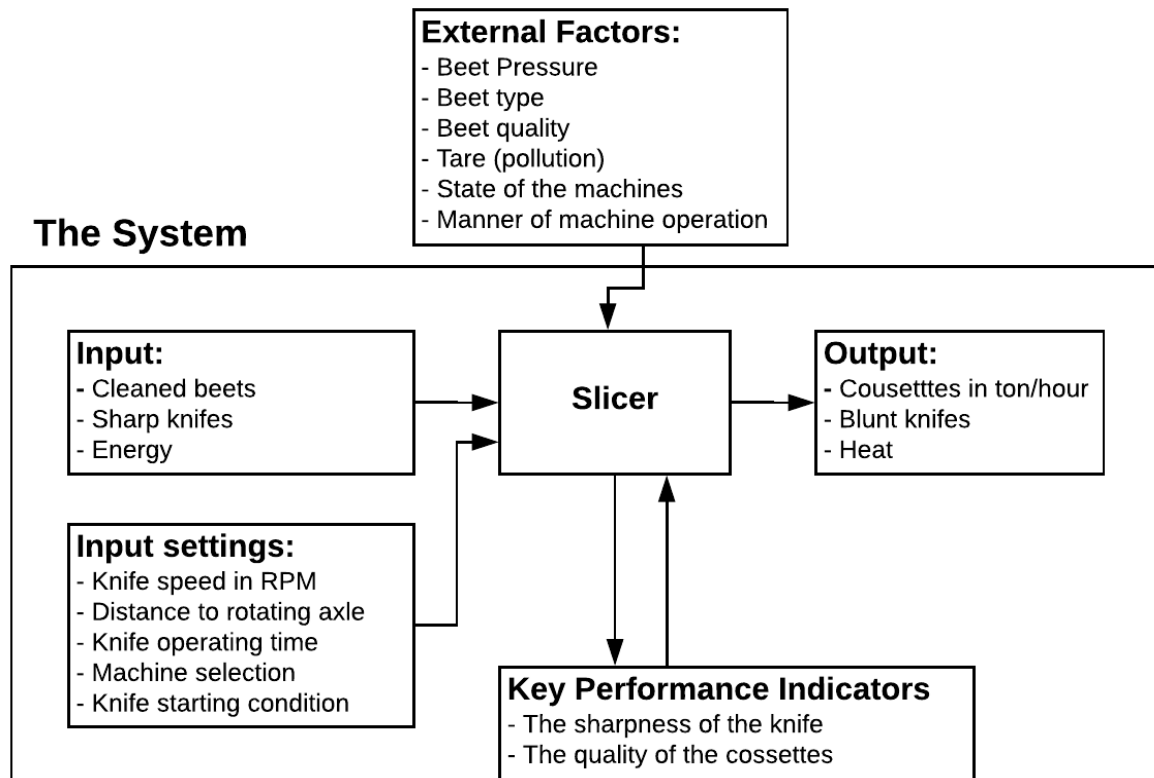


Figure 4: Conceptual model of the slicer - Focus of paragraph 1.3

### 1.3.2 Input, input settings and output

Figure 4 displays how cleaned beets, sharp knives and energy are transformed into cossettes, blunt knives and heat. The output can be controlled by the input settings.

The knife speed depends on the number of revolutions per minute (RPM) and it is currently unknown if there is a relation between the RPM and the knife deterioration. Another observation is that the cossette quality drops if the RPM gets higher and Appendix A5 explains a higher RPM causes production stops due to mush.

The distance to the rotating axle determines the angular speed because knives are placed side by side in a knife block (Figure 5). The distance from the axle causes a 60% difference in angular speed. It is unknown if knife sharpness deterioration is related to the different angular speed or the geometry of the cutter.

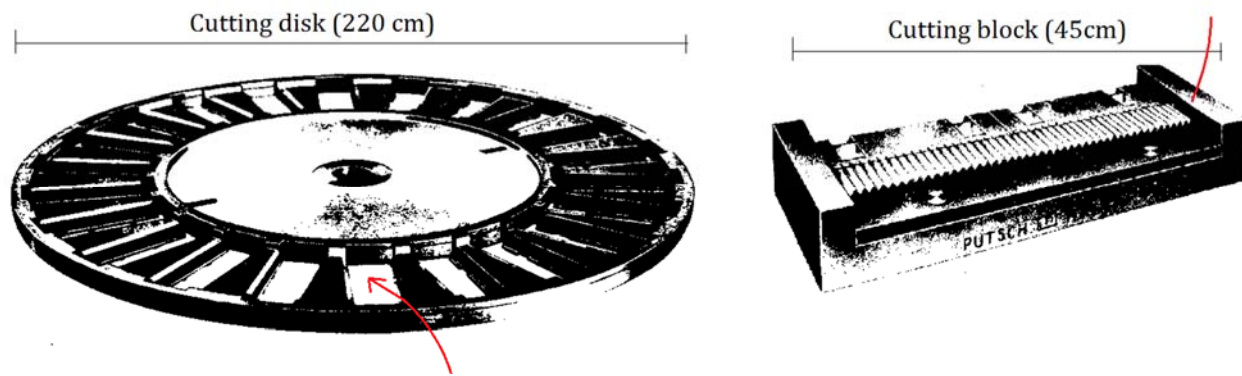


Figure 5: A cutting disk is placed horizontally in a slicer. Each cutting disk contains 24 knife blocks. Knife blocks can be removed from the slicer to change the two 20cm wide knives with sharp knives.

The lead time of a knife is typically 20 hours. No information is available on the knife sharpness deterioration speed and what type of regression can be observed.

The machine selection refers to the location underneath the beet bunker (Appendix B1). The beet bunker is a temporary storage directly above the 15 slicers and contains cleaned beets. Machine operators mentioned slicers placed underneath the center of the beet bunker experience more knife sharpness deterioration because more debris and tare is concentrated in the middle of the beet bunker. No objective knowledge on the performance of individual slicers exists.

Each slicer starts with sharp knives. Knives used at Viervelaten can be brand new or sharpened by the factory. It is unknown if there is difference between the knives. Furthermore, the fraiser used for sharpening is replaced after each day (850 knives) due to wear. Differences in fraiser wear and differences in the placement of the fraiser in the grinding machine can result in variable sharpness.

### 1.3.3 External factors

The external factors of the system (Figure 4) influence the output but contrary to the input variables, the external factors are not controllable during the beet campaign. The beet bunker is filled at a constant level of 8 meters to insure a constant beet pressure onto the cutting disks. The beet type, tare and quality varies from one hour to the next as described in Appendix A1.

### 1.3.4 Key Performance Indicators

The KPI's of the system are the sharpness of the knife and the quality of the cossettes.

**Knife Sharpness:** An assumption is made that knives entering the machine have equal sharpness. During the typical 20 hour of operation a slicer cuts 1600 tons of beets of which 32-64 kg is tare as described in Appendix A3. Tare, debris and the beets cause the knives to become blunt over time.

**Cossette Quality:** The only person who continuously monitors the state of the cossettes is the control room operator. This is explained in Appendix A4.

### 1.3.5 Cossette quality and characteristics

Cossettes quality is affected by uncontrollable and controllable variables. As a result a slicer can one moment produce good quality cossettes, and bad quality cossettes ten minutes later with the exact same machine settings. The uncontrollable variables are associated with the fact that it is a “nature product”. The variables for measuring the quality of the cossettes can therefore not easily be quantified. Multiple methods are used to determine the quality of the cossettes. A method is selected depending on its purpose. The book Sugar Technology (van der Poel, Schiweck, & Schwartz, 1998a) and the book Beet-Sugar Handbook (Asadi, 2006) describe four measurements which can be used to describe cossette quality.

- Silin number (SN): The length of 100 gram cossettes. Acquiring the SN number requires to lay out a random sample of 100 grams lengthwise. Good quality cossettes SN: 10 - 18.
- Mush content (MC): the weight percentage of cossettes smaller than 1 cm in a 100 gram cossettes sample.
- Slab content: the weight percentage of slabs in a 100 gram cossette sample. Slabs are cossettes that are still connected to multiple other cossettes due to incorrect slicing. Good quality cossettes have a combined MC and Slab Content lower than 5%
- Swedish number. (SWN) A ratio formed by the weight of cossettes longer than five centimetre divided by the weight of mush from the same sample. Good quality cossettes have a SWN higher than ten.

At Vierverlaten the cossette quality is determined by factory performance changes and by manual inspection.

- Slicer RPM: The slicers require a higher RPM to maintain the target throughput if knives turn blunt during production.
- Slicer torque: The torque of the slicers however drops over time.
- Juice Pump power: Appendix A5 provides the function and location of the juice pump in the production process. When the filter of the diffusion tower gets clogged up, the juice pump requires more power.
- Manual inspection: The control room operator personally inspects the cossettes by touch for elasticity and by eyesight for geometry, mush and slab content.

The beet sugar handbook describes ideal characteristics for cossettes:

- Uniform width (3 to 6 mm thick, square or V (roof-like) shape)
- Uniform length (30 to 60 mm long)
- Minimal amount of fines (no value is mentioned)
- Minimal amount of slabs (no value is mentioned)
- Non-mushy texture



The Vapro documents of Vierverlaten are handbooks developed for training purposes. The Vapro documents contain information related to machine settings and production methods used at Vierverlaten. In contrary to the beet sugar handbook the Vapro documents state slabs are necessary to increase the upward flow in the diffusion tower and mention an accepted upper limit of 10% (weight percentage of total cossettes).

The book Sugar Technology describes the V shaped geometry of cossettes are created by alternating A and B knives as demonstrated in Figure 6. If beets move during cutting or if the knives blocks are not correctly aligned or not placed in alternating order, less ideal shapes are created. The ideal shape (Type-1 shape from Figure 7) has a high surface area and a constant thickness. In reality this shape is rarely seen. Type-3 and Type-4 are the most common geometry.

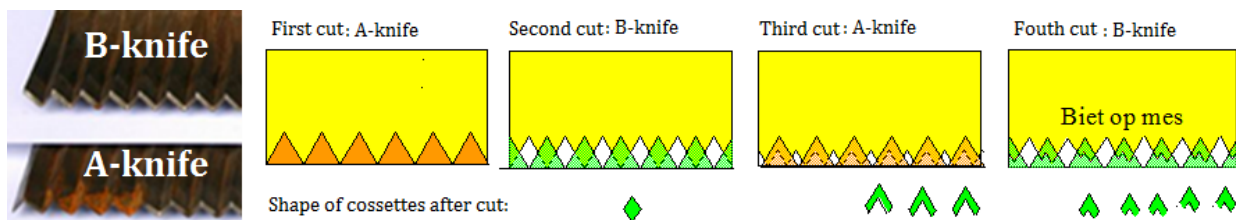


Figure 6: The A and B knives have a triangular wave pattern. The wave pattern of B-knives are shifted half a period with respect to the wave pattern of A-knives. Knife blocks containing either A-knives or B-knives are placed in alternating order to create V shaped cossettes in four consecutive cuts.

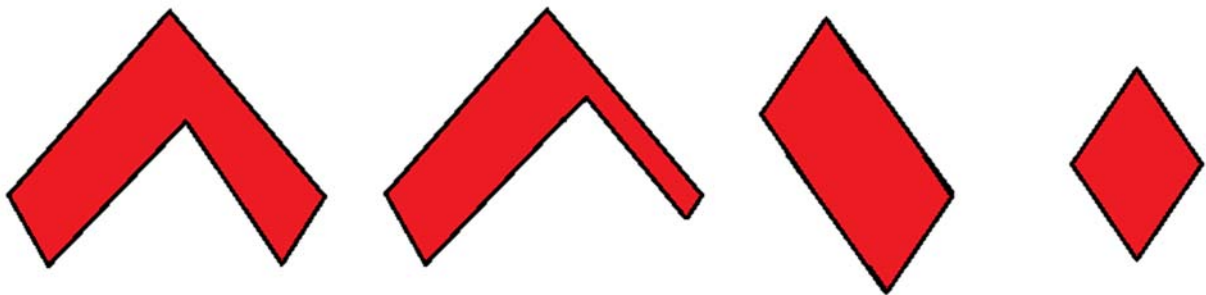


Figure 7: Cross-sectional view of the different cossette geometries produced by a slicer. From left to right: Type-1, Type-2, Type-3 and Type-4. Type-1 is ideal but in reality non-existent. The type-3 and type-4 are produced at Vierverlaten.



## **1.4 STAKEHOLDER ANALYSIS**

The main source of information for machine settings is acquired from employees at Volverlaten. It is therefore essential to know the division of tasks and the additional stakes. The next paragraph describes the task division during the 2017/2018 campaign. The stakeholders mentioned are restricted to the system discussed in the conceptual model.

The plant manager is responsible to meet the throughput targets set in collaboration with upper management focused on cost efficient diffusion. Main decisions on machine settings are the responsibility of the plant manager. Higher throughput of the frontend factory for example, can be reached by increasing the RPM of the slicers which causes more mush. Appendix A5 explains how mush causes the filter of the diffusion tower to get blocked. This however can be solved by increasing the knife height. Plant manager: "We aim for one blockade per twenty four hours in order to make sure we do not cut cossettes to coarse". The plant manager mainly works during day time, but is on call around the clock.

The shift manager oversees the current state of the production. There are over 500 variables that cause variations in the throughput. The responsibility of the shift manager is to oversee settings concerning machines, valves and pumps are constantly tweaked to reach the throughput targets provided by the plant manager.

The control room operators have a room in the middle of the factory containing over thirty monitors that display a schematic layout of the factory with real time information on the most vital variables. The control room operator judges the quality as mentioned in the previous paragraph and determines when and which slicer needs knife replacement.

The machine operator performs the actual change of the knives as explained in appendix A4. When the control room operator requests a knife change it can take up to two hours for the knife change to take place if the machine operator is occupied with other tasks.

## **1.5 THE RESEARCH OBJECTIVE**

The conceptual model points out that knife sharpness and cossette quality are key performance indicators of the system. A technique to indicate the performance of the system through cossette quality, is to determine the SN, SWN, MC and slab content. However, because these methods are designed for manual analysis this is not applicable in real time. The quality control methods used at Volverlaten (section 1.3.5) are not ideal. First, the throughput sensor measures the combined throughput from all the slicers in a line (Appendix B), thus the RPM is not related to the performance of an individual slicer. Secondly, each slicer row is connected to a separate juice production station which has an additional 110 minutes lead time. Furthermore, the manual quality control performed by the control room operator is performed 3-6 times per shift. Manually determining the quality of cossettes is not an objective method and shift change every 8 hours.

The current goal of Volverlaten is to accurately determine which slicer is up for a knife change in order to improve the cossette quality. In 2017 an external company (Axians) created a prediction model to determine which slicer should be replaced. Axians created deep learning algorithms that analysed data on machine performance (Slicer RPM/Torque). A deep learning prediction model can only be as good as the data it is provided with. Because the knife replacements recorded in the factory database were decided upon with the constraints

mentioned in the previous paragraph (no individual slicer performance, lead time of 110 minutes and no objective cossette quality control) and the fact that the cossette quality is related to external factors, the prediction model reached an accuracy of 60%.

Knife sharpness is the other performance indicator of the system. If knife sharpness can be objectively determined by a machine without human intervention it can be implemented as performance indicator. In an ideal situation only controllable variables exist enabling, each variable to be quantified and a knife sharpness deterioration prediction model can be created. Thus, if the external factors (Figure 4) at Vierverlaten can be neglected an accurate prediction model should be feasible. Real time knife sharpness is not available, thus knives have to be analysed after they are used for production. To side-line the effect of external factors the slicers have to be operated multiple times according to a set of specified input settings.

**Therefore the research objective is to find out how a knife sharpness measurement can be created for the non-straight edge knives used at Vierverlaten to quantify the input variables.**

The required accuracy of the sharpness measurement is related to the acceptable time a knife will perform after its lead time. For a lead time of 1200 minutes (20 hours) a sharpness resolution of 0 (infinitely sharp) to 100 (acceptable bluntness level is exceeded), will result in a prediction model that can accurately distinguish knife sharpness for between each 12 minutes of production since  $1200(\text{minutes})/100=12(\text{minutes})$ . 10 to 15 minutes is the average time the machine operator needs to prepare for a knife change. Therefore acquiring a resolution of 1:100 is the goal for the creation of the prediction model. Throughout this research the required resolution will be referred to as (1:100).

## **1.6 RESEARCH QUESTIONS**

To achieve the research objective two main questions have to be answered:

- **How can a knife sharpness index for non-straight edge knives be defined?**
- **How can data of a knife analysis be used to develop a prediction model for knife sharpness deterioration?**

## 1.7 RESEARCH DESIGN AND STRUCTURE

The goal of the research is to find out whether knife sharpness measurement can be created for the non-straight edge knives. The empirical cycle (Figure 8) as proposed by Wieringa (Wieringa, 2014) is implemented since it fits the knowledge oriented goal of this thesis.

In the first chapter the problem background is discussed and analysed using a conceptual model to determine the research goal. The research goal and research questions state a knife sharpness index is required for the non-straight edge knives used at Vierverlaten.

Chapter two provides finding of academic literature about knife sharpness and the different applications of knife sharpness. Currently no literature discusses the knife sharpness and knife sharpness index (KSI) of non-straight edge knives. Three methods for straight edge knives are selected for verification and require the calculation of the Fracture toughness of a substrate. No literature describes how the fracture toughness can be acquired using a non-straight edge knife.

Chapter three verifies the usability of each method for non-straight edge knives. One of the three methods is not applicable for the user case of the non-straight edge knives of the factory. The chapter concludes with the research setup for the other two methods.

Chapter four contains the results of the research followed by the discussion, the conclusion and ends with recommendation for further research.

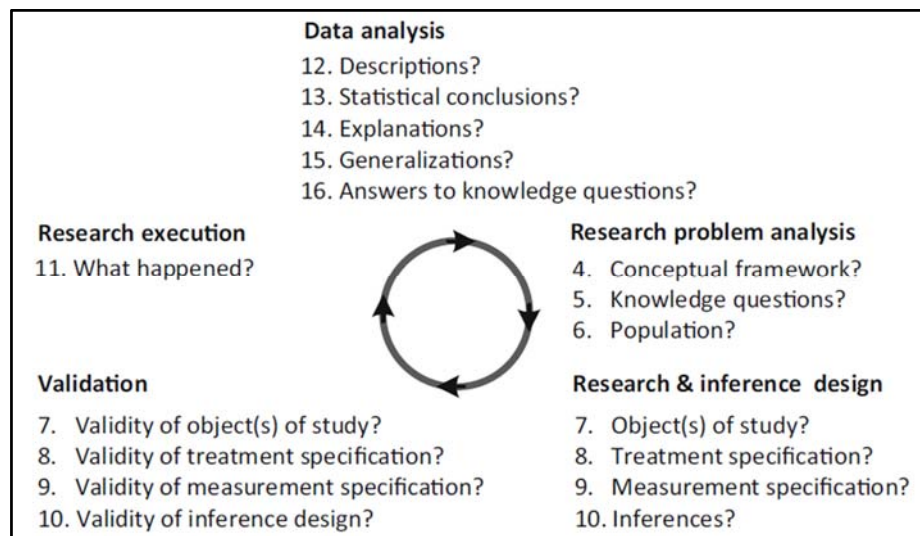


Figure 8: The empirical cycle as proposed by Wieringa to conduct knowledge based research. (Wieringa, 2014)

## 2 THEORETICAL BACKGROUND

---

Section 2.1 distinguishes different applications of knife sharpness. The differences between optical and mechanical sharpness measurement techniques are discussed in section 2.2. Methods to analyse the non-straight edge blade used at Vierverlaten (section 2.3) are discussed in section 2.4. The chapter concludes with three potential parameters that require validation before test results can be generated.

### 2.1 GENERAL APPLICATION OF KNIFE SHARPNESS

The term blade and knife are both interchangeably used throughout the literature, knife sharpness will be used throughout this thesis. A knife is a tool with a cutting edge or blade. A blade is the portion of a tool, weapon, or machine with an edge that is designed to puncture, chop, slice or scrape surfaces or materials.

Due to the broad application of knives and their sharpness index user case, different industries developed multiple knife sharpness measurements and parameters. This research focuses on the knife sharpness related to cutting soft solids and/or organic materials. Literature on knife sharpness is the most common in: surgical knife sharpness, forensic medicine, meat processing and food processing.

Literature for surgical knives focuses on the creation of thin knives with smoother surfaces, to reduce wound tissues formation caused by tearing and snatching (Tsai et al., 2012). A direct connection between the knife sharpness and tissue trauma regeneration is proven in an article from 1985 (Marks & Black, 1985).

Forensic medicine as explained in the book by (Saukko & Knight, 2015) is related to forensic pathology. It uses knife sharpness as a tool for cut analysis, and the dynamics of stab wounds (O'Callaghan et al., 1999).

Ergonomics in the meat processing businesses became a popular topic after the US Labor department acknowledged the risk factors for musculoskeletal disorders in distal upper extremities (MSDUE) to be 30 times greater than the industry average. (United States Department of Labor. Bureau of Labor Statistics, 2001; Werner & Franzblau, 2018). The literature focuses on ergonomics and the relation between knife sharpness and the cutting forces experienced by the wrist of the knife user.

In the food processing industry, knife sharpness is related to quality of the product and trends such as increased forces resulting from higher speeds and lower temperatures (Schuldt, Arnold, Kowalewski, Schneider, & Rohm, 2016)(Brown, James, & Purnell, 2005)(Portela & Cantwell, 2001a).

## 2.2 SHARPNESS DETERMINED THROUGH OPTICAL AND MECHANICAL TECHNIQUES

A review article on knife sharpness by Reilly explains that the knife sharpness parameter of different industries are derived through either optical or mechanical techniques (Reilly, McCormack, & Taylor, 2004).

For optical sharpness analysis detailed information on the knife geometry is acquired through analysing close-up images of the knife tip (Figure 9). The following parameters are acquired through observation: knife wedge angle (degrees), blade tip radius ( $\mu\text{m}$ ) and offset ( $\mu\text{m}$ ). Furthermore, the knife sharpness can be analysed in finite element methods (FEM). A FEM research by McCarthy discusses how knife sharpness is affected by its wedge angle and its tip radius (McCarthy, Ní Annaidh, & Gilchrist, 2010). McCarthy stresses the limitation of FEM: it does not model the actual cutting process since advanced fracture and compression mechanics on Nano scale would be required. Furthermore, mechanical blade analysis is much more sensitive to detect wear than optical analysis and thus more capable to detect differences in knife sharpness (Schuldt, Arnold, Roschy, Schneider, & Rohm, 2013).

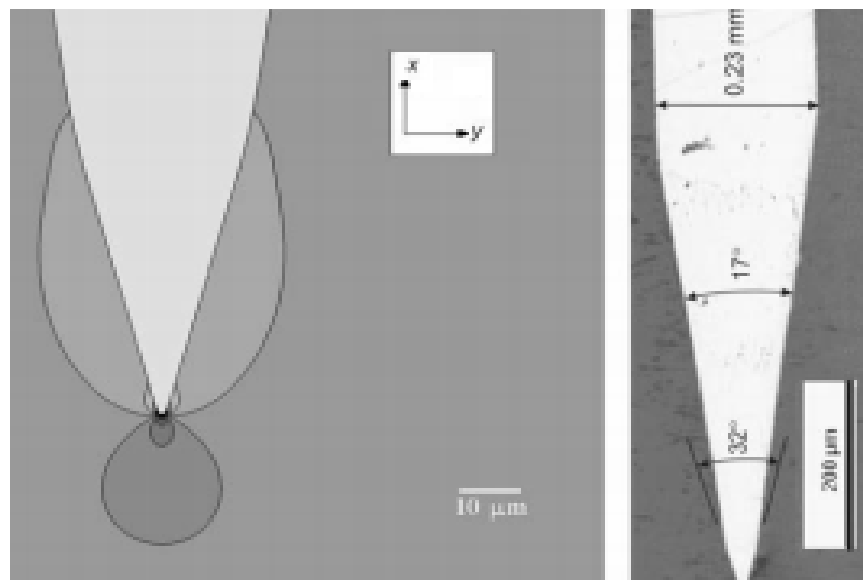


Figure 9: (left an example of a finite element analysis model containing the forces around the tip. Right) Optical image analysis (McCarthy et al., 2010).

Mechanical sharpness analysis is performed through cutting tests and force measurements. Because of different applications, different knife sharpness analysing methods are successfully applied throughout the literature. The force on the substrate and the grip force during cutting (McGorry, Dowd, & Dempsey, 2005)(Marsot, Claudon, & Jacqmin, 2007), the force required to initiate cutting (Portela & Cantwell, 2001b), the cut depth, the cut initiation depth and or the cutting moment (in Nm) (Verhoeven, Pendray, & Clark, 2008)(Zhou & McMurray, 2009), are examples of knife sharpness benchmarks.

McCarthy recognized the need for standardization of a mechanical knife sharpness parameter and developed the Blade Sharpness Index (BSI) (McCarthy, Hussey, & Gilchrist, 2007a). Because the BSI is independent of the cutting speed, substrate type and substrate thickness it can be used to objectively compare different knife types. However, if the friction force in a measurement is low compared to the fracture toughness, the BSI may not be a reliable standalone parameter (Schuldt et al., 2016) (McCarthy et al., 2007a).

### 2.3 NON-STRAIGHT EDGE KNIFE SHARPNESS

Vierverlaten uses non-straight edge A and B knives (Figure 10). The knife has a tip radius of 0.2 mm. The tip wedge angle is 35 degrees. At  $x = 1.5(mm)$  the wedge angle changes to 10 degrees. At  $x = 9.1(mm)$  the knife the wedge angle changes to 0.0 degrees, the knife is straight. Knives replaced by the machine operator go to the sharpening facility. In the sharpening facility they are first realigned. In the second step the 10 degree wedge angle is sharpened followed by the 35 degree wedge angle. Knife weight is related to the number of times it is sharpened. A new knife weighs 598 grams and used knives can weigh just over 450 grams and be 10(mm) shorter in the x direction.

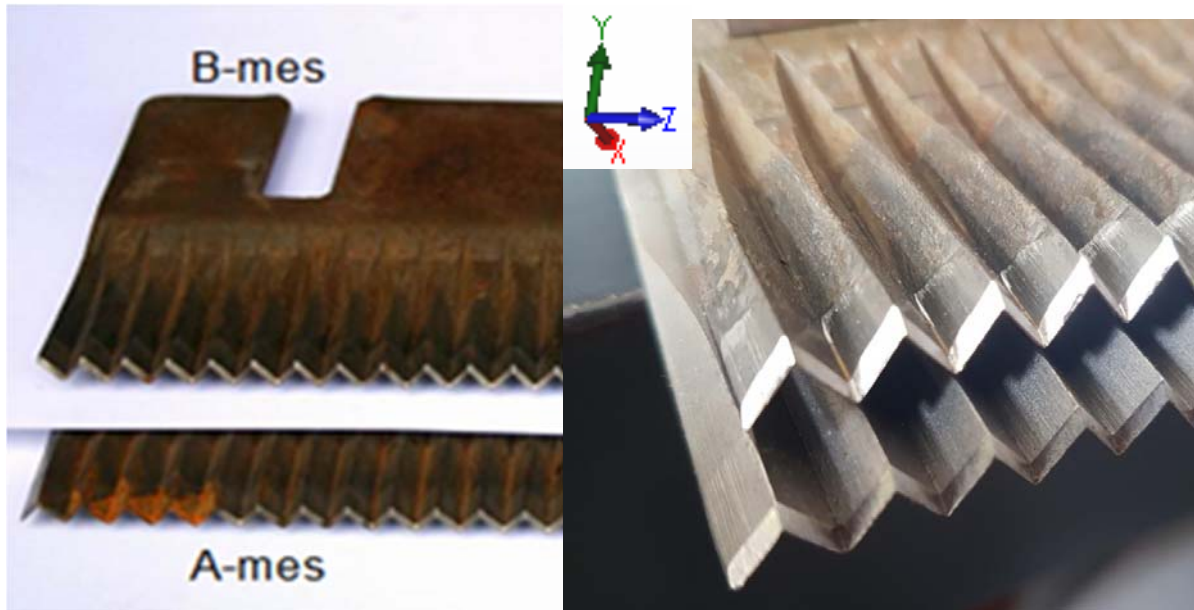


Figure 10: (Left) Image of an A and B knife used at Vierverlaten. Type-A and type-B knives alternate each other to create Type-4 V shaped cossettes. (Right) A close-up of a new knife at the bottom and a sharpened used knife on top, where it is clearly visible that the surface roughness of the used knife highly increases after 9.1 mm of indentation.

The blade of a straight-edge knife runs along the z axis in the x, y, z plane, whereas the blade of a non-straight-edge knife does not. As can be seen in Figure 10 the blade edge of the knife type used at Vierverlaten follows a triangular wave pattern along the z-axis. The non-straight edge blade requires specialized sharpening tools and are therefore uncommon and non-existent in the literature. Furthermore, the sharpness of the knives at Vierverlaten is increased by single edge sharpening at the cost of durability while the knife design also has a high wedge angle to increase durability and lower knife sharpness (McCarthy et al., 2010). Due to these characteristics, the knife sharpness cannot be acquired by replicating a measurement technique as described in literature.

## 2.4 MEASUREMENT TECHNIQUES

Three measurement techniques described in the literature are of significant relevance to design a usable sharpness parameter for this research.

- Indentation parameter
- BSI parameter
- Cut initiation parameters

Measurement limitations observed from Figure 10 are the maximum indentation of  $x = 20.0(mm)$  for a sharp knife due to the end of the triangular pattern. As mentioned in section 2.3 the knife can be 10mm shorter at the end of its lifetime thus comparing knives allows the maximum indentation  $x = 10.0(mm)$ . Furthermore, the transition from the second wedge angle to no wedge angle at  $x = 9.1(mm)$  may contaminate the research findings. In conclusion, a maximum indentation of 9.1(mm) can be applied to both sharp and blunt knives.

### 2.4.1 Indentation parameter

The indentation parameter is created by orthogonally applying a knife to a substrate and measuring the indentation (mm). Each repetition uses a different knife, the same amount of potential energy, and a fresh substrate of equal size and structure. Higher indentation indicates higher knife sharpness. The indentation parameter is a potential candidate due to the simplicity of the technique.

Data for the indentation parameter is acquired by repeating the drop test for a knife until the average indentation depth is constant. The maximum allowable travel distance into the substrate is 9.1 mm thus in order to acquire the required resolution (1:100), measurements have (McCarthy, Hussey, & Gilchrist, 2007b) to reach an accuracy of approximately 0.1mm (McCarthy, Hussey, & Gilchrist, 2007c).

### 2.4.2 Blade Sharpness Index parameter

Taking into account the ratio between the substrate friction forces and the fracture toughness of the substrate (section 2.3), the BSI is also a potential candidate and can be calculated using eq.1.

The force while steady state cutting refers to Figure 11d where the knife is suspended in the substrate. Due to the large size of the factory knives this parameter is harder to acquire. However, the force and indentation depth at cut initiation (Figure 11a) do not share this problem. Therefore the cut initiation parameters are also potential candidates.

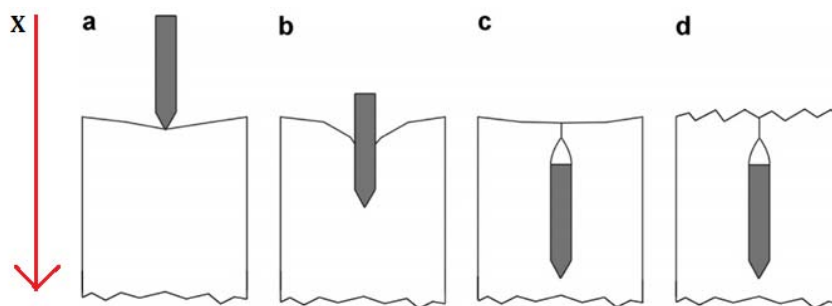


Figure 11: Cross sectional schematic image of a straight edge knife during different stages in the cutting process. (a) Cut initiation moment, (b) Just after cut initiation the substrate material travels up the side of the blade, (c) the moment at which the material re-joins and the whole knife travels through the substrate, (d) Steady state cutting through a material

The BSI parameter can be acquired according to the method described by (McCarthy et al., 2007a) where a knife cuts into a substrate with constant speed while measuring the force. The BSI formula reads:

$$BSI = \frac{\int_0^{\delta_i} F(x) dx}{\delta_i \times J_{Ic}}$$

Where  $\delta_i$  is the distance  $x$  (mm) a knife travels from the first contact with the substrate until the moment cutting initiates.  $F(x)$  Is the force in Newton measured at  $x$  (mm) indentation and  $J_{Ic}$  is the fracture toughness  $kJ/m^2$  of the substrate. The fracture toughness of the substrate material has to be determined for each type of substrate. According to a method described by (Atkins, 2005), the fracture toughness of a material can be acquired with data of the cutting forces. The articles by McCarthy (McCarthy et al., 2007a) successfully applied the method. The fracture toughness  $J_{Ic}$  is acquired from the data of a cutting test when steady state cutting is observed. The formula reads:

$$J_{Ic} = \frac{(X - P) \times u}{A_{knife}}$$

Where  $X$  (N) is the force read while steady state cutting a substrate.  $P$  (N) is acquired by performing a second cutting test where the knife is run through the previously cut substrate. Since the substrate is already cut only the friction force will impede the knife. Now  $(X - P)$  is the force required for cutting.  $u$  (mm) is the millimetre of indentation and  $A_{knife}$  ( $mm^2$ ) is the surface area of contact between the knife and the substrate. Note that the contact surface area is zero until cutting initiates.

The test of Schuldt and McCarthy to determine the fracture toughness estimated steady state cutting for straight-edge knives to initiate around 10mm when the knife wedge angel is 0. For the knives used at Vierverlaten the fracture steady state cutting have to be observed while cutting the second wedge angel due to the restrictions discussed in the beginning of section 2.4.

### 2.4.3 Cut initiation parameter

As explained in Section 2.4.2, the cut initiation depth and force are also required to determine the BSI. Therefore only two measurement methods have to be applied and the cut initiation parameters can be read from the data.



### 3 VERIFICATION OF KNIFE SHARPNESS METHODS

---

Different knife sharpness parameters and methods were discussed in chapter two. It was also concluded that no existing sharpness methods were applicable to the non-straight edge knife used at Vierverlaten due to its geometry and measurement constraints. Section 3.1 verifies the indentation method, and section 3.2 verifies the BSI method. The chapter concludes with the verified parameters for the research setup.

#### 3.1 INDENTATION METHOD

The difference between the highest indentation ( $mm$ ) of a sharp knife and the lowest indentation ( $mm$ ) of a blunt knife divided by 100 is the required accuracy. Due to the indentation limit of 9.1 mm, advanced measurements are required.

First, a simplified concept model was built where a knife was applied to a rotating arm with an intended accuracy for individual tests of 0.5( $mm$ )(Figure 12). Air friction is neglected due to the low speeds involved and mechanical friction at the hinge is neglected due to the total weight of the arm compared to the potential friction energy at the hinge. To ensure objective measurement a mechanical trigger initiates the drop test.

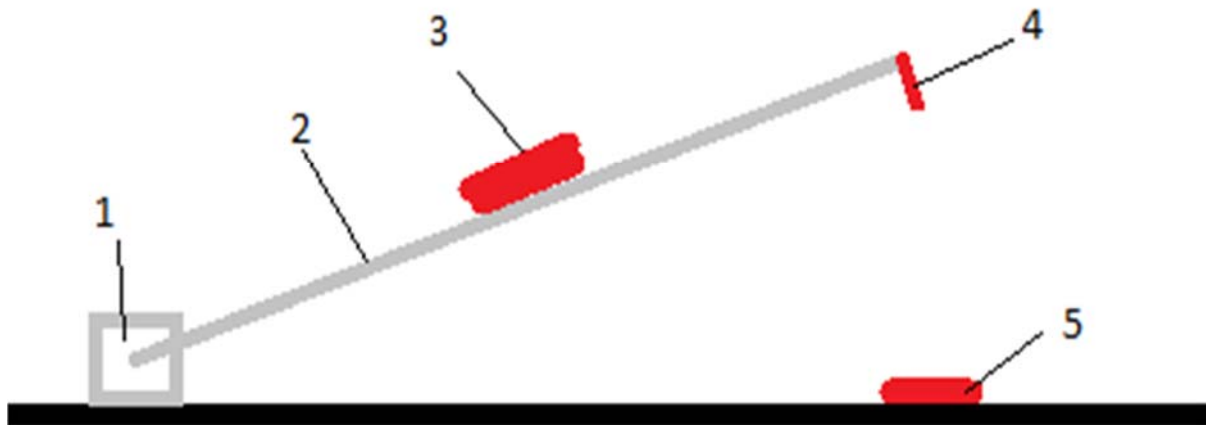


Figure 12: Schematic image of the concept setup to verify the indentation parameter. An arm (1) is connected to a hinge (2) with the knife (4) attached at the other end. A movable weight (3) is used to control the potential energy at user specified drop heights. The indentation into the substrate (5) measured in mm is the parameter indicating the sharpness of a knife.

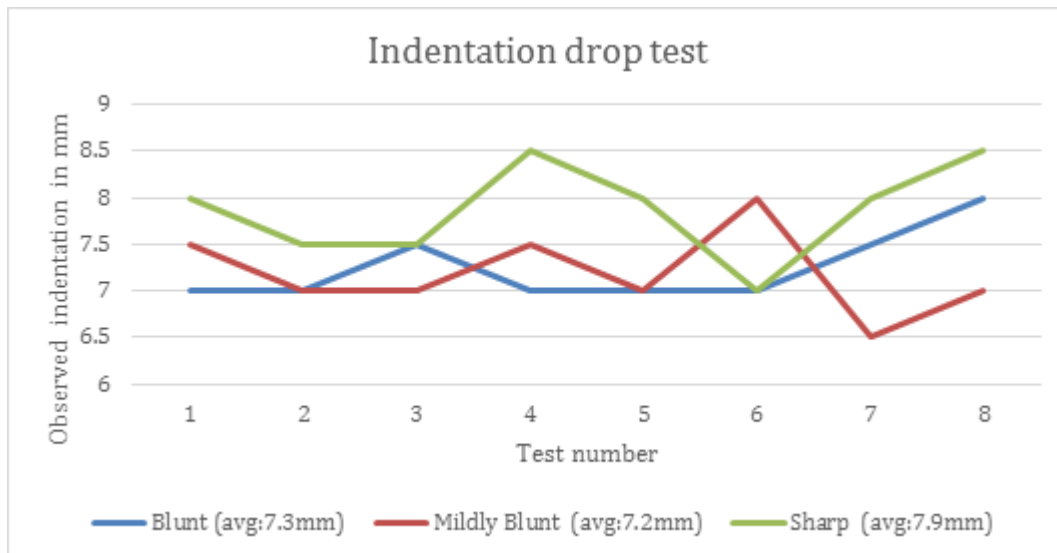


Figure 13: The results of the concept cutting test including the average (avg.) indentation.

Substrate indentations under 9.1mm were measured with the correct placement of the movable weight, a potential energy of 1 Joule and a drop height of 10cm. Results shown in Figure 13 prove that a difference in indentation depth for a sharp and blunt knife can be observed. The average indentation depth for a sharp knife is  $x = 7.9(mm)$ , followed by  $x = 7.3(mm)$  for the blunt knife while the indentation depth for the mildly blunt knife is an unexpected  $x = 7.2(mm)$ . The observed difference in average cut depth between a sharp and blunt knife is  $0.6(mm)$ . Therefore an advanced setup requires accurate measurement readings within 6 micro meters.

Due to the high standard deviation, the incorrect reading for blunt and mildly blunt knives and the required accuracy, the indentation method is deemed unfit to analyse the non-straight edge knives used at Vierverlaten.

### 3.2 BSI METHOD

The method described by (McCarthy, Hussey, & Gilchrist, 2007d) can be executed using the material test system 810 (MTS810) as displayed in Figure 14. The MTS810 can record force in micro Newton, time in microseconds and distances in micro meters. The machine is available at the University of Groningen and is currently setup to measure forces up to 15 000 Newton with a testing range of 150mm. In order to measure the knives with the MTS810 special clamps were designed using SOLIDWORKS. 3D printed polymer clamps are not an option due to the high clamping force of the MTS810 (25000 Newton). Therefore the clamps were created using the metal machining facilities at Viervelaten.

Before measurements and analysis related to the input variables could be performed, several parameters that could influence the results were examined.



*Figure 14: Photograph of the machine (MTS810) used for the cutting trials*

- Substrate type: Schuldt calculated the BSI for several types of food and stated that the substrate friction force should be high compared to the fracture toughness of a substrate (Schuldt, Arnold, Kowalewski, Schneider, & Rohm, 2016). Potato is therefore chosen as a substrate.
- Speed: with high friction and low cutting speed, stick-slip can occur where the substrate movement along the knife (in opposite direction of cutting) becomes incremental. Furthermore, lower speeds may increase the precision of the test results. Test are required to determine the right speed.
- Substrate width: The blade sharpness of a straight edge blade is determined at a single point. Knife sharpness may vary on different parts of the knife and a bigger substrate may result in a more constant sharpness measurement.
- Number of measurements: in an ideal situation each repetition gives the same results. The organic nature of potatoes might result in differences between tests. Therefore the number of measurements required to reach the accuracy (1:100) has to be verified.

In an ideal situation each of these four variables can be tested for at least 6 different settings and benchmarked against each other. Performing a total of  $4^6 = 4096$  unique tests is not realistic. Furthermore, the limited availability of the MTS810 requires assumptions and testing in several runs to efficiently use the available time.

### 3.2.1 First test run and data processing

In the first test run the substrate type was verified. A brand new sharp knife was used and the graphed raw data is displayed in Figure 15. The following settings were applied:

- Substrate: Potato
- Speed: 0.5 (mm/s)
- Substrate width: 60 (mm)

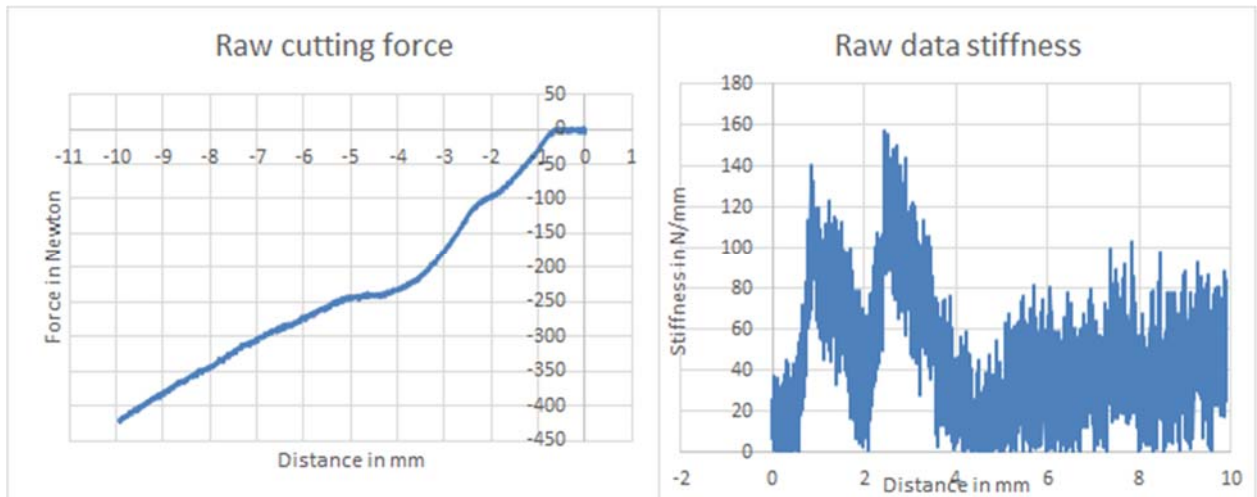


Figure 15: Raw graph from the data the MTS810 machine produces. The method described in section 3.2.1 transforms the data of each test to usable data as can be seen in Figure 17.

The MTS810 creates a raw data file for each test contains three columns: a column for the measured force( $N$ ), a column for the distance( $mm$ ), and a column for the expired time( $seconds$ ). A graph of the raw data is shown in Figure 15. Before test results can be compared, data sets have to be normalized and corrected for certain errors.

The first five recorded data points are neglected since they are used to accelerate the machine to the desired speed. It was observed that the number of incorrect data points due to acceleration was similar for all the speeds used throughout this research.

The distance and the force are recorded negative because the software of the MTS810 is currently setup for stretch testing while cutting is a form of compression testing.

The MTS810 is calibrated between tests and the exact point of contact (between the knife and the substrate) has to be determined for each test. The data observed in Figure 15 between -1.0 ( $mm$ ) and 0.0 ( $mm$ ) corresponds to the travel time of the knife to the substrate. The initiation of the climb towards the first peak in the stiffness graph determines the first contact with the substrate.

The distribution of observed stiffness values (Figure 15) before knife-substrate contact is displayed in Figure 16 and are corrected by applying a moving average. A moving averages smoothest out trends from past information using their average; a moving average of the past eight values did not alter the final results beyond the required accuracy. And the moving average of eight lowers the stiffness standard deviation from 10.2 ( $N/mm$ ) to 2.2 ( $N/mm$ ) while the maximum deviation decreased from 44 ( $N/mm$ ) to 13 ( $N/mm$ )

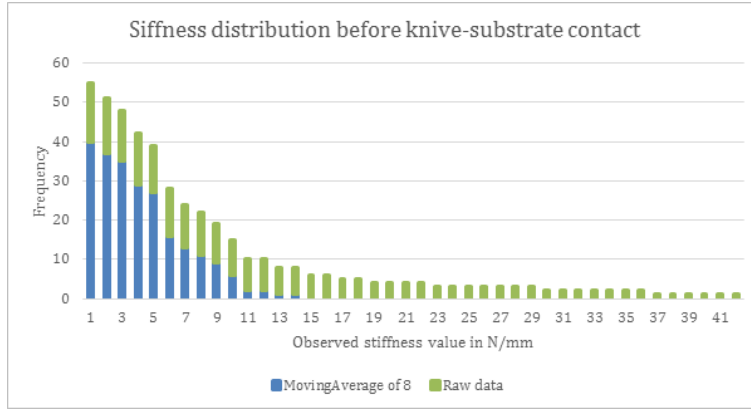


Figure 16: Distribution of the stiffness while the knife is traveling towards the substrate.

### 3.2.1.1 Substrate type verification

The results of the first test with correction are shown in Figure 17. Point A marks the start of the indentation test and corresponds to the first observation of a stiffness value greater than 13.0 (N/mm). Point B corresponds to the point at which the compression energy in the substrate is released and cutting initiates. After point B the substrate starts to travel up the knife (Figure 11b) due to the energy stored from indentation without cutting. At point C the substrate has restored to normal position and for a knife with one wedge angle, steady state cutting would start to initiate. The second wedge angle enters the substrate at point D and causes another increase in stiffness because the growth of the cross sectional surface area of the knife increases. Between point E and F the average stiffness is 10 (N/mm) and cutting is assumed to be constant. After point F, the knife reaches the end of the substrate and rupture of the substrate can occur. The BSI requires the measured force(N) and indentation depth(mm) at cut initiation (point B), and the force while steady state cutting. The potato substrate can be used to determine these values.

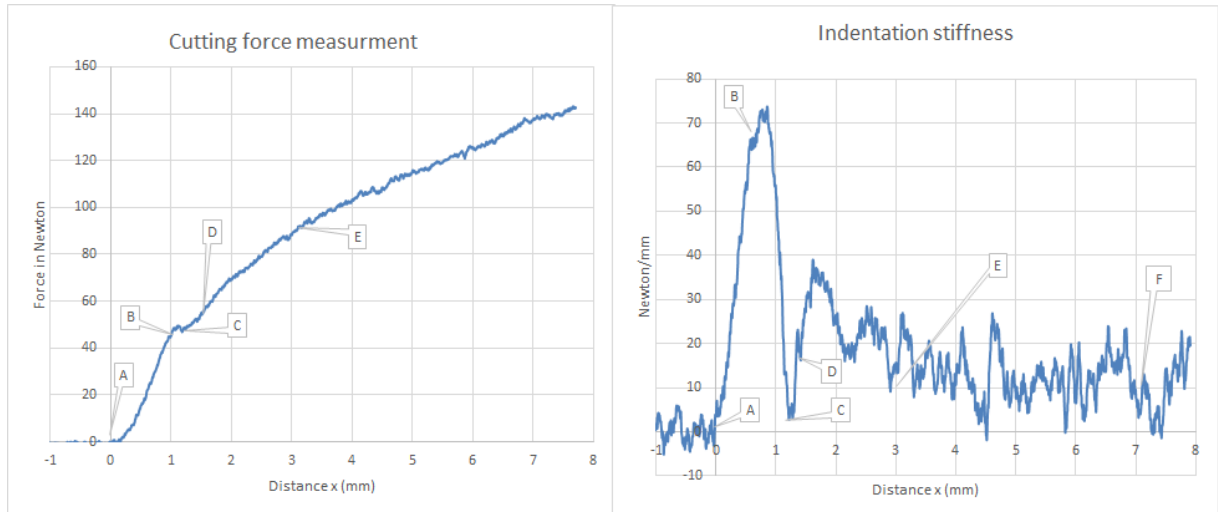


Figure 17: Data graphs from the first cut test. A new factory knife (Figure 10) is used to cut through a horizontally placed  $60 \times 10 \times 10 \text{ mm}^3$  potato substrate with 0.5 mm/s. (A) The point of contact between the knife and the substrate. (B) The point at which cutting initiates. (C) The point at which normal cutting continues (D) The point at which the second wedge angle enters the substrate. (E) Steady cutting through the substrate. (F) Continues steady state cutting.

### 3.2.2 Second test run: Speed and substrate width

#### 3.2.2.1 Indentation speed verification

In the second test run a sharp knife was tested at different cutting speeds and for different substrate widths. The following settings were applied:

- Substrate: Potato
- Speed: 0.1 (mm/s)- 0.25(mm/s)- 0.5 (mm/s)- 1.0 (mm/s)
- Substrate width 60 (mm)

At all three speeds the point and force at cut initiation could be read from the data. The standard deviation of the cutting force and stiffness while steady state cutting from  $x = 6.5(\text{mm})$  to  $x = 7.0(\text{mm})$  are similar at all three speeds. Cutting at 1.0 (mm/s) resulted in a table with 1000 data points. Cutting with a speed of 0.1 (mm/s) resulted in 10000 data points. The extra data points create additional accuracy to 0.001 mm between each value. The level of accuracy is not required but also does not influence the test results. The use of 0.25 (mm/s) does not add extra research time since several preparations have to be completed between tests. Therefore 0.25 (mm/s) is used for all tests after the third test run.

#### 3.2.2.2 Substrate width verification

The following settings were applied:

- Substrate: Potato
- Speed: 0.5 (mm/s)
- Substrate width 10(mm), 40(mm), and 60 (mm)

Three different substrate widths were tested two times each because a wider substrate has a bigger contact area and is therefore expected to provide less deviation in result. Results for all six tests are shown in Figure 18. Cutting test 1 and 2 performed with a 60(mm) wide substrate show different results for the force (N) and cut indentation depth(mm). Cutting test 3 and 4 performed with a 40(mm) wide substrate also show different forces (N) and cut indentation depths(mm). However, the measured force(N) and indentation depth(mm) for test 5 and 6 performed with a 10(mm) wide substrate do show comparable results.

A possible explanation for the deviant results of test 1 to 4 can be related to the substrate type. Potato is a natural product and each part of a potato differs in structure. The observed similarity in test 5 and 6 contradicts this explanation. Even though the six tests were performed with different parts of different potatoes, the 10 (mm) wide test substrates were prepared simultaneously resulting in an equally sized potato parts, while the 40 (mm) and 60 (mm) substrates were not prepared simultaneously.

The fact that test 1 and 2, and 3 and 4 show dissimilar results is not related to the substrate width but rather the method of substrate preparation. The fact that successful data was create with a substrate width of 10(mm) concludes additional substrate width is not necessary. Section 3.2.3 discusses the aforementioned differences related to substrate preparation.

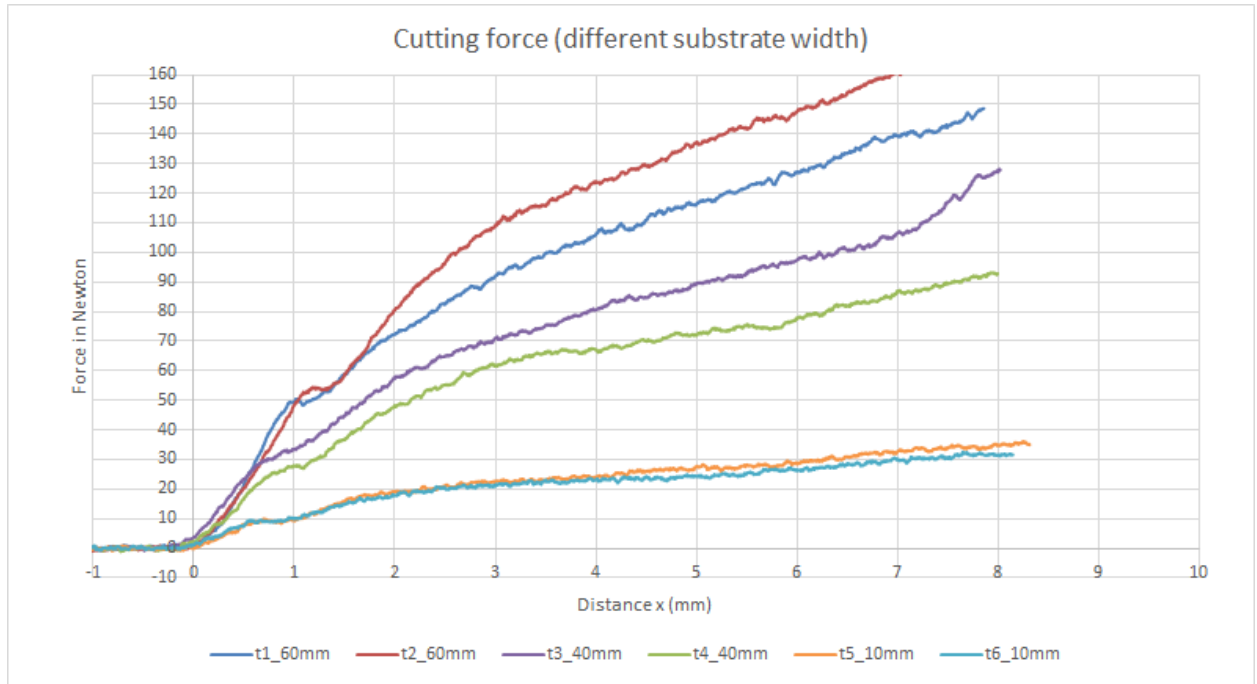


Figure 18: Graph containing six cut tests. A new factory knife (Figure 10) is used to cut through horizontally placed potato substrates with 0.5 mm/s. The highest two graphs cut through a  $60 \times 10 \times 10 \text{ mm}^3$  substrate, the middle two graphs cut through a  $40 \times 10 \times 10 \text{ mm}^3$ , and the lower two graphs cut through a  $10 \times 10 \times 10 \text{ mm}^3$  substrate.

### 3.2.3 Third test run: Comparing knives

In the third test run a blunt, a mildly blunt and a sharp knife were tested and the required number of test per knife are analysed.

#### 3.2.3.1 Number of test required per knife for sharp and blunt knives.

The following settings were applied:

- Substrate: Potato
- Speed: 0.5 (mm/s)
- Substrate width 60 (mm)

Two tests were executed with a blunt knife and four tests were executed with a mildly blunt knife (Figure 19). A clear distinction between the blunt and the mildly blunt knife can be seen in Figure 19: less force is required to cut using a mildly blunt knife. The observed differences showed in the graph of Figure 20 are related to the dimensions of each substrate.

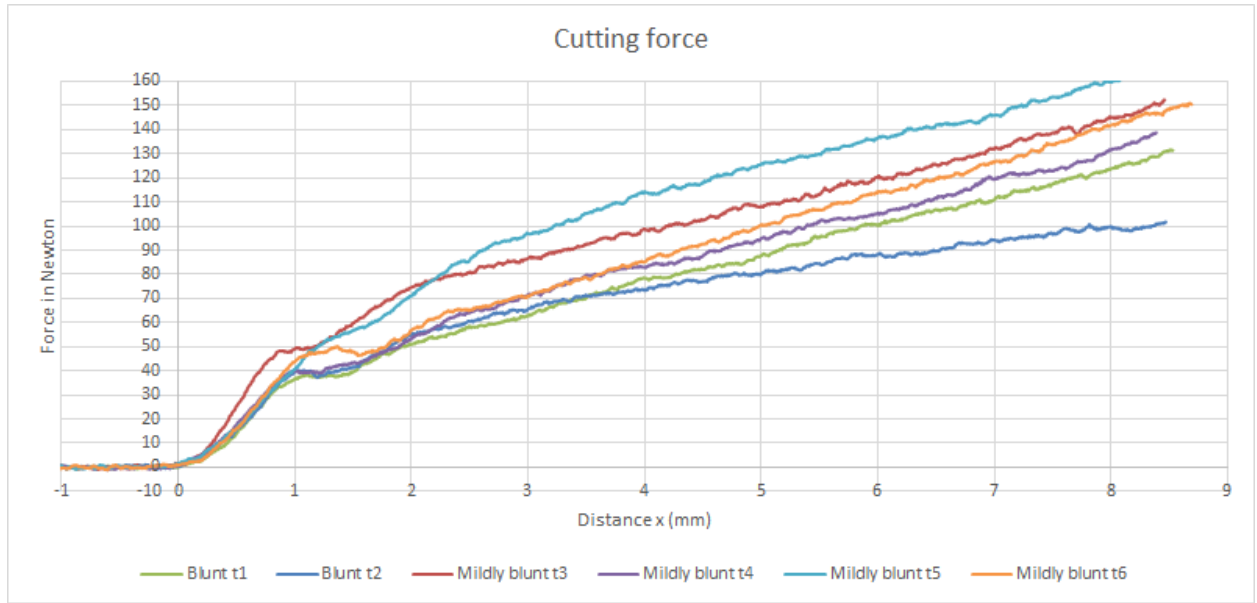


Figure 19: A blunt and a mildly blunt knife are tested 2 and 4 times.

Similar results are expected when repeating a cutting test with the same knife and equal settings. This is tested for both a sharp, a blunt and a mildly blunt knife. Results presented in Figure 20 show different values of the cut initiation forces and indentation depths for all tests. Cutting errors of 0.3 (mm) lead to oversized  $60.3 \times 10.3 \times 10.3 \text{ mm}^3$  substrates that have an initial side pressure due to the dimensions of the clamp ( $10 \times 10 \times 10 \text{ mm}^3$ ), undersized substrates measuring  $59.7 \times 9.7 \times 9.7 \text{ mm}^3$  can move during measurement. The standard deviation is greater than 19%, therefore concluded that applied force differences when preparing the substrates by hand also contaminate the result if cutting is performed simultaneously.

It was concluded that more than five repetitions are required for each test because of the size difference in the potato substrates. For further testing a polymer substrate is used that does not require manual substrate cutting.

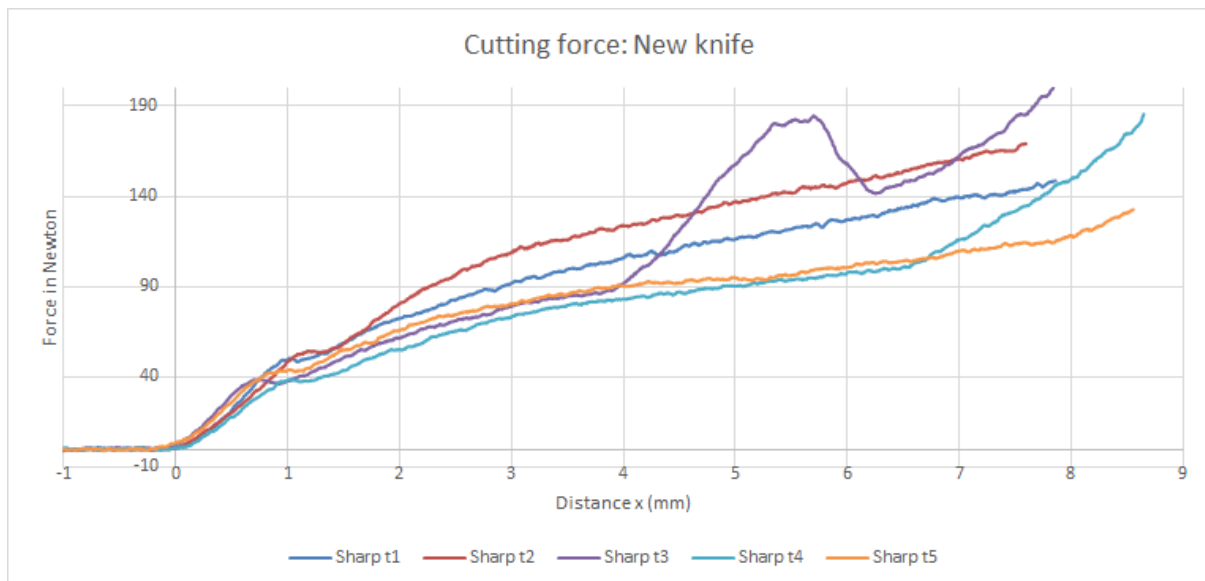


Figure 20: Five cut tests are performed with a new sharp knife. Results should be similar but they are not because test results from manually preparation of substrates are not objective.



### 3.2.4 Fourth test run: Polymer substrate

The following settings were applied:

- Substrate: Potato
- Speed: 0.25 (mm/s)
- Substrate width 12 (mm)

The differences in potato substrate size lead to inaccurate measurements. A polymer substrate is used to create objective measurements. Similar results are expected when the test is repeated with the same settings. A new sharp knife was tested three times and the results are displayed in Figure 21. For these tests the cutting speed was lowered to 0.25mm/s because it provided higher resolution and did not add additional research time. From the three tests the observed standard deviation while steady state cutting is 3.8%. The force required for 8 (mm) indentation of a blunt knife was found to be 40% higher than a sharp knives. Therefore it was concluded that the polymer can be used to benchmark knives.

## 3.3 APPLIED RESEARCH SETUP

The MTS810 is used to analyse the knives. The cutting speed of 0.25 (mm/s)s was used to cut a polymer substrate with a maximum indentation of  $x = 9.1(mm)$ . Due to the limited available time the number of tests per knife is two.

The research setup is verified. Section 3.4 explains how the knives were selected for each input variable.

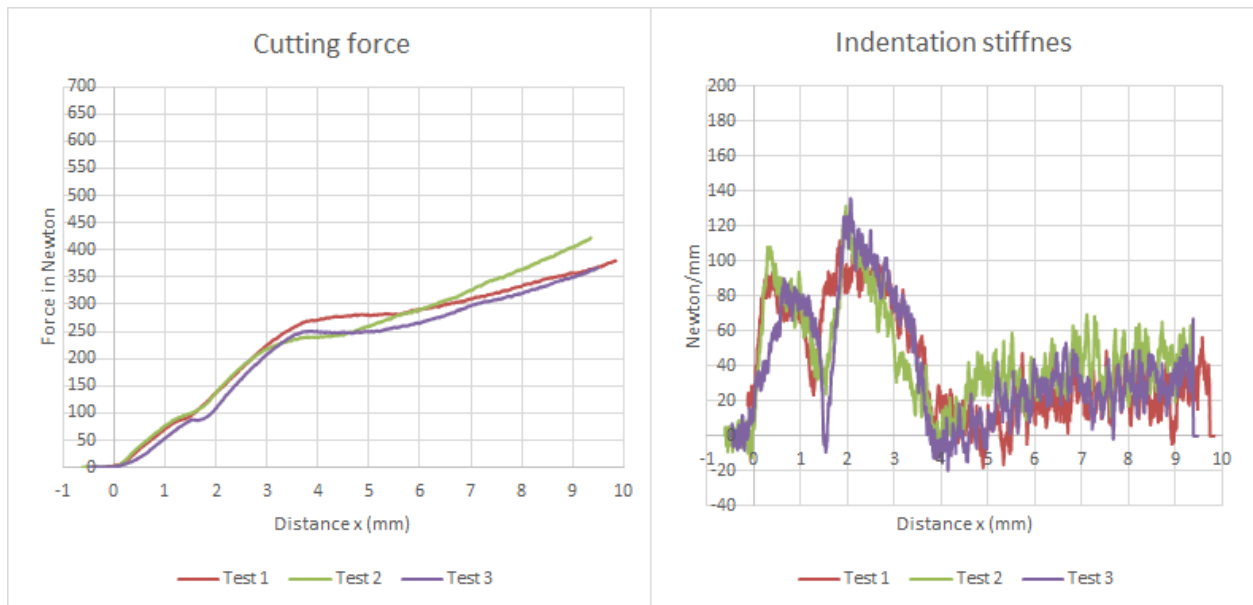


Figure 21: A new sharp knife is used to cut through horizontally placed substrates with 0.25 mm/s. The first tests with the polymer show that the required data contains the points required to calculate the BSI. Repetition of the test show similar results.

### 3.4 KNIFE COLLECTION

In order to measure differences in knife sharpness related to a specific input variable, knives have to be operated under specific settings while eliminating external factors that can contaminate the results. This results in several general knife collection constraints:

- The input changes from one hour to the next (Appendix A2) thus measurements for each variable have to be performed simultaneously.
- Comparing knives from different slicers requires that the knife operating time is equal and that the applied RPM is also equal. Thus knives have to be collected from the same row (Appendix A4).
- It is unknown if there is a difference between a factory reshaped knife or a brand new knife. Due to the required number of knives and the availability of brand new knives, factory sharpening knives have to be used. To overcome possible difference in factory sharpened knives due to fraiser condition and fraiser installation, knives should be sharpened within a single day and preferably either at the end or at the beginning of a fraiser placement.
- Two knives are placed side by side as can be seen in Figure 5. Due to the rotational movement of the cutting disk the angular velocity is higher at a larger distance from the axle. Therefore only the knives placed furthest from the axle should be compared.
- Finally, no extra interference from external factors or changes in machine settings can be allowed during operations.

#### 3.4.1 Elimination of external factors

Within the constraints mentioned in section 3.4 knives were collected (and ladled for later use) for each of the input variables.

- Knife speed in RPM: The RPM of the slicers used at Vierverlaten is determined by the capacity set point (Figure 5) and for safety reasons a custom RPM could not be applied. It was possible to compare two neighbouring slicers from a separate rows with an RPM of 25 and 37.
- Distance to the rotating axle: two knives are placed on a rotating cutting disk (Figure 5). Knives were collected from a slicer running at 37 RPM. At 37 RPM the knife part closest to the rotating axle has an angular rotation speed of  $9.09\text{km/h}$ . The knife part furthest from the rotating axle has a 62% higher angular speed of  $14.66\text{km/h}$ .
- Knife operation time: the general lead time of a set of knives is 20 hours. For this test knives were collected from the same slicer running at 35 RPM at operation times of 3, 6, 12, 18 and 24 hours. At the specified times two knife blocks were replaced.
- Machine selection: Control room operators observe the cossette quality is lower for slicers placed underneath the middle of the beet bunker. To compare the different performance of slicers all the knife blocks of 4 slicers in a row were changed within one hour. After a simultaneous production of 20 hours knives were gathered from each of the slicers.
- Initial knife sharpness: Knives sharpened directly after fraiser replacement and knives directly before fraiser replacement were collected and compared with a brand new knife.

In the next chapter the data will be analysed, the BSI will be created and the input variables as mentioned in the conceptual model will be examined.

## 4 RESULTS

Chapter 4 shows results, observations and conclusions as far as they can be directly drawn from the results. Results are discussed in chapter 5.

Section 4.1 contains the fracture toughness and the BSI. Section 4.2 and 4.3 are used to examine the usefulness of the BSI as a standalone parameter. Section 4.4 compares other parameters extracted from the data to benchmark the results of the input variables mentioned in the conceptual model. The chapter end with an answer to the research questions in section 4.5.

### 4.1 FRACTURE TOUGHNESS AND THE BSI

Fracture toughness is determined as described in paragraph 3.2. Figure 22 shows the graphs of the first pass (X), the free pass (P) and the net force (X-P) of the polymer. The fracture toughness is determined from Figure 22 at steady state cutting. As observed steady state cutting occurs between 6 and 8mm indentation. Eq.2 is used to calculate the fracture toughness for the polymer ( $J_{Ic} = 2.959 \text{ kJ/m}^2$ ) and for the potato ( $J_{Ic} = 0.405 \text{ kJ/m}^2$ ). The fracture toughness is used in Eq.1 to calculate the BSI for the test results displayed in Figure 23.

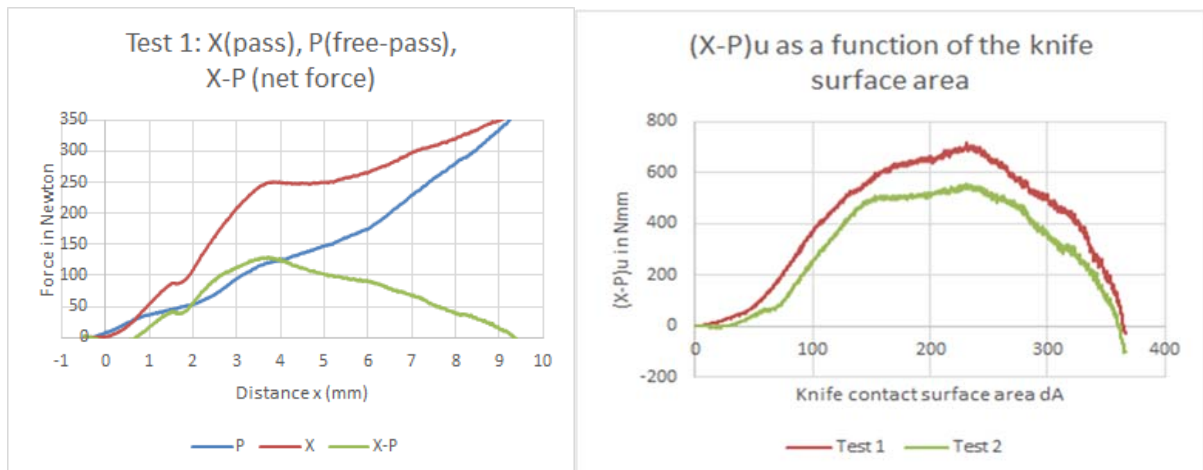


Figure 22: The left graph contains the cutting force of, P the first pass through a polymer substrate, X the free pass through the same substrate, and X-P the net graph that displays the cutting force without friction. The right graph contains the results corrected for the knife surface area A from Eq.2

The table in Figure 23 contains the BSI of a sharp factory knife for two different substrate types and two different substrate sizes. The average BSI is 0.25 and has a standard deviation of 0.066. The Table in Figure 23 shows the observed BSI is acquired for a sharp non-straight edge knife and is independent of the substrate type and substrate width. Therefore it can be concluded that the BSI can be acquired for a knife with a non-straight edge blade.

In order to reach the required accuracy (1:100). The observed BSI standard deviation of 0.066 requires the BSI of a blunt knife to be at least 6.66 (a hundred times greater than the BSI of a sharp knife)

Substrate	Width (mm)	Test nr.	Cut initiation energy (Joule)	Cut initiation depth $\delta_i$ (mm)	Cut initiation force (F)	Fracture Toughness $J_{Ic}$ kJ/m <sup>2</sup>	BSI	Avg. BSI
Polymer	12.00	1	1.58	0.21	10.80	2.96	0.21	0.24
		2	2.35	0.26	16.54	2.96	0.26	
		3	4.08	0.46	17.58	2.96	0.25	
	24.00	1	7.84	0.35	40.74	2.96	0.32	0.28
		2	8.71	0.53	40.93	2.96	0.23	
	60.00	3	5.22	0.67	20.97	0.41	0.32	
Potato	60.00	1	1.27	0.32	6.03	0.41	0.16	0.20
		2	1.29	0.41	11.16	0.41	0.13	
		3	5.22	0.67	20.97	0.41	0.32	
	10.00	1	0.20	0.15	0.76	0.41	0.32	0.28
		2	0.11	0.12	2.41	0.41	0.24	

Figure 23: The BSI of a sharp factory knife measured multiple times for different substrates and substrate widths.

## 4.2 BLUNT KNIFE ANALYSIS

Figure 24 compares the results of a new knife and a blunt knife. The blunt knife is used for 20 hours at 37 RPM in a cutter with an average throughput of 80 tons/hour. In contrast to the findings of Schuldt and McCarty (Schuldt et al., 2016) (McCarthy et al., 2007a) a lower BSI was measured for the blunt knife. Furthermore, the standard deviation of the sharp knife is 0.066 while the BSI of a blunt knife is just 0.12. The high standard deviation confirms the previous findings: the BSI is not accurate enough to compare the non-straight edge blades of the factory knives as a standalone parameter. The other parameters however show a clear distinction between a sharp and blunt knife. The cutting force in Figure 25 corresponds to the test results from figure 24. Until  $x = 4.0(mm)$  similar behaviour is observed for the sharp and the blunt knife. If  $x > 4.0(mm)$  steady state cutting initiates with 25 (N/mm) and 75 (N/mm) for the sharp and blunt knives. Furthermore, a maximum force of 316N and 528N for the sharp and blunt knives at  $x = 8.0(mm)$ .

The cut initiation parameters are inconsistent for both knives. The BSI does not use any data after cutting is initiated and Figure 25 shows the required cut initiation force of the sharp knife is higher than the cut initiation force of the blunt knife. As previously explained the blunt knives used for this research started as a factory sharpened knives and not as new knives. Section 1.3.2 explains the fraiser (Figure 3) is replaced every day due to wear. Section 4.3 compares a new knife, a knife sharpened after fraiser replacement and a knife sharpened before fraiser replacement.

Test	Test nr.	Cut initiation energy (Joule)	Cut initiation depth $\delta_i$ (mm)	Cut initiation force (F)	BSI	Force x=3mm	Force x=5mm	Force x=8mm	Stiffness 0.75-1.0 (N/mm)	Stiffness 3-4 (N/mm)	Stiffness 6-7 (N/mm)
Sharp	1	1.576	0.213	10.797	<b>0.208</b>	225.673	280.363	315.480	76.903	45.528	20.168
	2	2.347	0.257	16.537	<b>0.257</b>	218.137	259.439	316.674	73.344	21.410	25.972
	3	4.080	0.463	17.577	<b>0.248</b>	209.294	249.606	295.036	74.938	40.314	29.478
Blunt	1	0.865	0.249	7.545	<b>0.098</b>	193.177	335.752	512.795	53.927	76.475	75.629
	2	1.406	0.291	12.248	<b>0.136</b>	208.009	357.812	528.278	61.407	81.402	75.745

Figure 24: Parameter comparison for a blunt and a sharp knife.

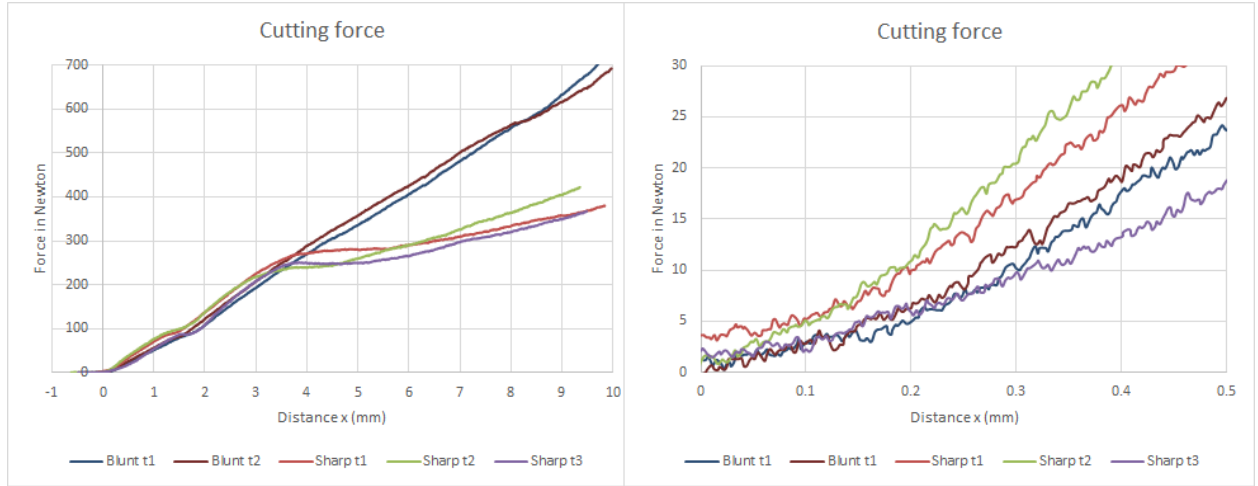


Figure 25: The polymer cutting force of a sharp and a blunt knife compared.

### 4.3 FACTORY SHARPENED KNIVES COMPARED

Figure 26 shows the BSI standard deviation for factory sharpened knives is 0.09, this is equal to the lowest measured BSI for a sharpened knife. This confirms that the BSI is not usable as a standalone parameter.

A clear distinction between a new blade, and a factory sharpened blades is seen at  $x = 3.0(mm)$  and  $x = 8.0(mm)$ . The observed cutting force at  $x = 3.0(mm)$  for a new knife, a knife after fraiser replacement and a knife before fraiser replacement are 218N, 170N and 196N. These force measurements suggest factory sharpened knives are sharper since less force is required to cut through the first part of the substrate. Furthermore, the knife sharpened directly after fraiser replacement is significantly sharper than the knife sharpened before fraiser replacement. At  $x = 8.0(mm)$  the average forces for a new knife, a knife after fraiser replacement and a knife before fraiser replacement are 309N, 342N and 375N. This suggests a new knife is sharper than a factory sharpened knife. Furthermore, a knife sharpened after fraiser replacement requires 15% more cutting force compared to a knife sharpened before fraiser replacement.

Because, the average standard deviation of the force at  $x = 3.0$  and  $8.0(mm)$  is lower than 5% and an average force difference greater than 15% between new and factory sharpened knives is measured at  $x = 3.0$  and  $8.0(mm)$ , it can be concluded that the geometry

Knife	Test nr.	Cut initiation energy (Joule)	Cut initiation depth $\delta_i$ (mm)	Cut initiation force (F)	BSI	Average BSI	Force x=3mm	Force x=5mm	Force x=8mm
New knife	1	1.58	0.21	10.80	0.21	0.24	225.67	280.36	315.48
	2	2.35	0.26	16.54	0.26		218.14	259.44	316.67
	3	4.08	0.46	17.58	0.25		209.29	249.61	295.04
After fraiser replacement	1	3.03	0.38	19.16	0.23	0.15	158.73	270.16	360.55
	2	1.71	0.39	11.86	0.12		186.49	268.30	335.58
	3	1.84	0.57	16.77	0.09		164.92	268.67	332.80
Before fraiser replacement	1	4.91	0.44	23.66	0.31	0.23	186.98	319.96	394.19
	2	1.70	0.35	14.28	0.14		205.13	296.30	356.07

Figure 26: Comparing cutting test parameter of a new knife, a knife sharpened after fraiser replacement and a knife sharpened before fraiser replacement

#### 4.4 QUANTIFYING KNIFE SHARPNESS VARIABLES

The previous analysis suggests that the data can be used to compare and quantify non-straight edge knives. To verify if this is indeed the case knives collected after 0, 3, 6, 11, 16 and 24 hours of production in order to quantify different levels of knife deterioration.

For this test the cut initiation depth, force and energy are again unusable due to a high standard deviation. As determined in section 4.3 the BSI cannot be used as a standalone parameter. Figure 27 shows the force measurements of the 10 knives and differences appear after  $x > 4.0(mm)$  when steady state cutting initiates. The standard deviation of the cutting force as a percentage of the maximum measured force decreases at higher indentation and is 7.6% at  $x = 8.0(mm)$ . Figure 27 displays the cutting force measured at  $x = 8.0(mm)$  plotted against the production times. The force plotted against the production hours shows that an increase of 77.0 N (23.1%) cutting force is required to cut with a knife that produced cossettes for 3 hours compared to the force of an unused factory sharpened knife. After three hours of production a linear trend is observed and each addition hour of production adds 5.2 N (1.5%) to the force required for 8.0(mm) cut indentation. 100% corresponds to the lowest force observed at  $x = 8.0(mm)$  of an unused factory sharpened knife after fraiser replacement.

The stiffness appears to have a higher standard deviation between different production times and a linear trend of 1.7 N/mm (4.6%) for each additional hour of production is observed. The energy required to cut  $x = 8.0(mm)$  shows 216 J (16.4%) more energy is required to cut with a knife that produced cossettes for 3 hours compared to an unused factory sharpened knife. An additional 15.6 J (1.7%) of energy is required to cut through  $x = 8.0(mm)$  for each additional hour of production.

The energy and force indentation appear to be linear in the form of  $P = P_{initial}(A\% + B\% \times h)$ , where  $P$  is the performance required to cut  $x = 8.0(mm)$  into the substrate,  $P_{initial}$  is the initial performance of an unused factory sharpened knife to cut  $= 8.0(mm)$ ,  $A$  is the initial increase in % after three hours of production,  $B$  is the hourly % increase for each additional hour of production  $h$ .

For the force ( $N$ ) the formula reads:  $F_{force} = F_{initial} \times (23.1\% + 1.5\% \times h)$ . And for the Energy (*Joule*) the formula reads:  $E_{energy} = E_{initial} \times (16.4\% + 1.7\% \times h)$ .

From these results it can be concluded that knife sharpness can be quantified. 4.4.1 To section 4.4.3 quantifies the angular cutting speed, the performance of different slicers, and the RPM.

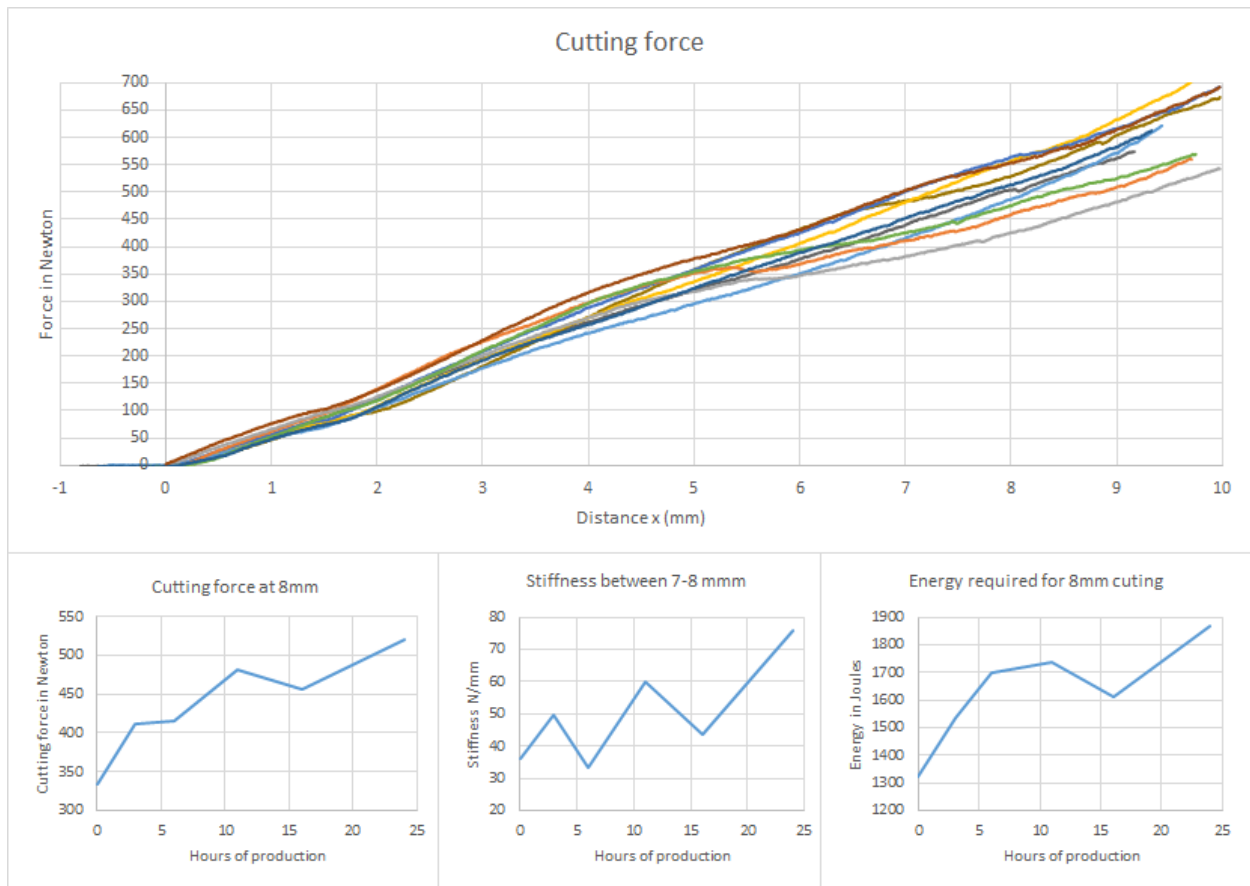


Figure 27: Cutting test performed on knives collected after 0, 3, 6, 11, 16 and 24 hours. Values for three parameters at  $x = 8.0(\text{mm})$  plotted against the hours of production.

#### 4.4.1 Difference cutting speed over 40cm blade (60%)

Section 1.3.2 explained the knife part closest to the axle rotates 60% faster than the knife part furthest from the axle and that higher speeds correspond to a higher throughput. Because the radius of the beets is approximately  $50.0(\text{mm})$  and the total knife width  $z = 400.0(\text{mm})$ , the knife was tested at  $z = 50.0(\text{mm})$  and  $z = 350.0(\text{mm})$ .

Figure 28 display the test results of two knives from the same machine. The tests results from  $z = 50.0(\text{mm})$  after 20 production hours show the cutting force at  $x = 8.0(\text{mm})$  is 0.8% lower than the cutting force of sharpened knife. However, the standard deviation is 7.5% and therefore it cannot be concluded that the knife at  $z = 50.0(\text{mm})$  is actually sharper than a factory sharpened knife.

At  $z = 350.0(\text{mm})$  the knife requires 30.2% more force to cut  $x = 8.0(\text{mm})$ , 5% more stiffness and 28.2% more energy compared to measurements at  $z = 50.0(\text{mm})$ . The observed energy and force differences appear to be more suited for comparing non-straight edge knives than stiffness measurements.

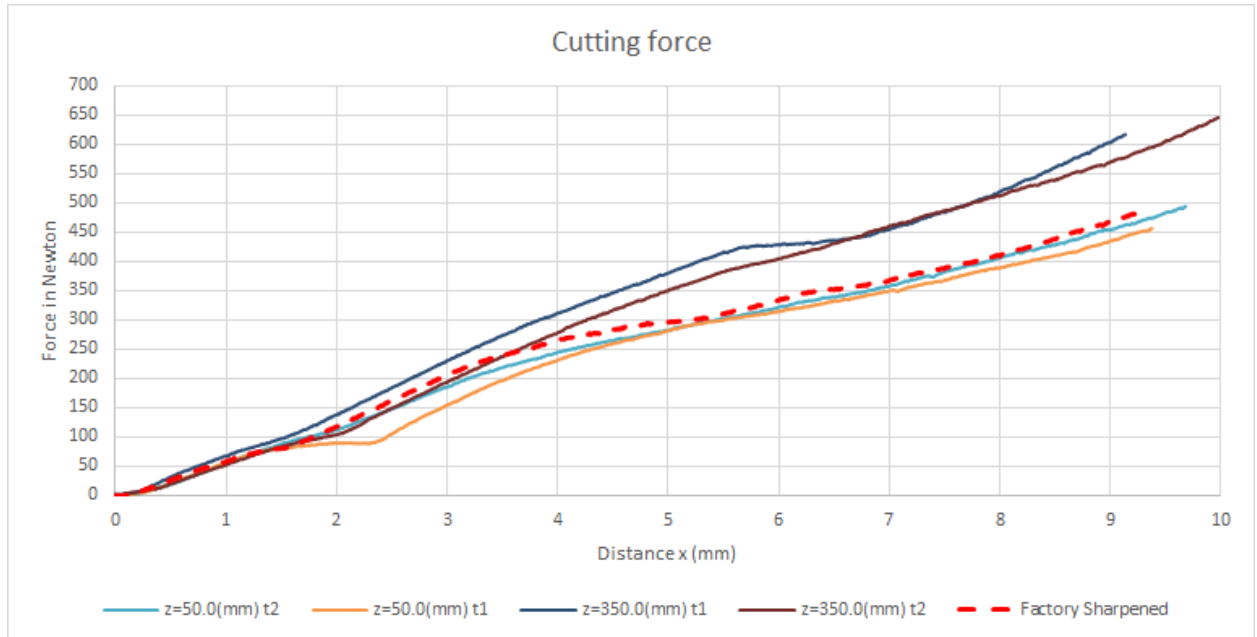


Figure 28: Comparing knife sharpness at different distances from the rotating axle.

#### 4.4.2 Location under Beet bunker

As mentioned in section 1.3.2 the observed cossette quality differs per slicer and presumably depending on the location underneath the beet bunker. Section 3.4 mentions knives from slicers in the bottom row are compared after 20 hours of simultaneous production. Figure 29 shows the result from the cutting test and the standard deviation at  $x = 5.0(mm)$  is 3.3% and 5.9% at  $x = 8.0(mm)$ . The standard deviation of the stiffness between  $x = 6.5(mm)$  and  $x = 7.0(mm)$  is 29.1%. The standard deviation from the energy consumption at  $x = 5.0(mm)$  is 4.5% and 6.5% at  $x = 8.0(mm)$ .

The average force of the slicers of the bottom row at  $x = 8.0(mm)$  is 503.1N. This is 42% higher than the force from a factory sharpened knife at  $x = 8.0(mm)$ . Results from section 4.4 show knives experiencing less sharpness deterioration are placed linearly across the 42% difference. It can be concluded that the knife deterioration is similar for all the slicers in the bottom row.

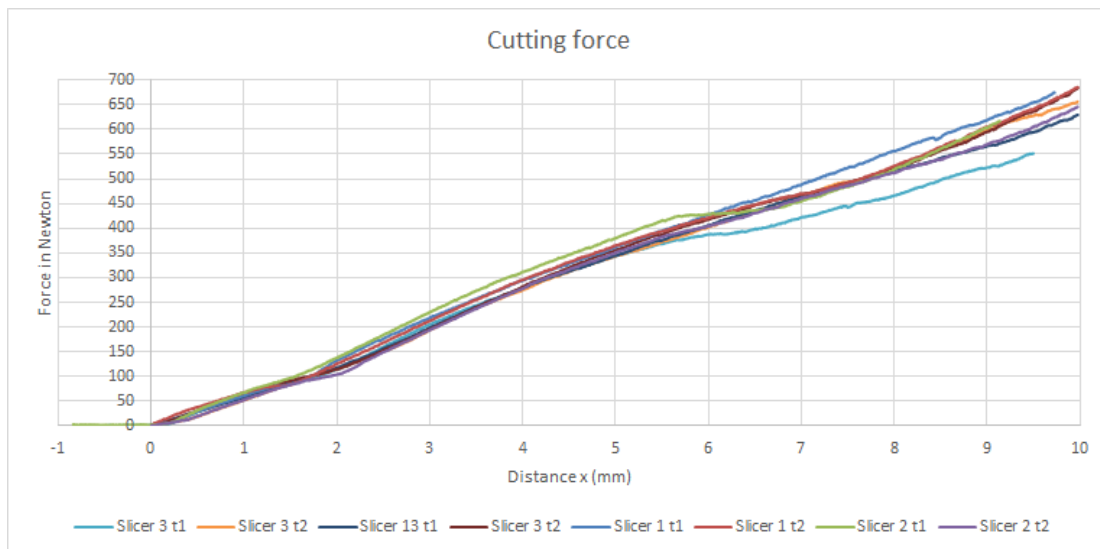


Figure 29: Comparing knives from four slicers in a row after 20 hour simultaneous production.



#### 4.4.3 Different revolutions per minute

Two slicers have run for 22 and 20 hours at 27 and 37 RPM. According to section 4.4, the two extra production hours should result in an additional 3.0% cutting force and 3.4% in cutting energy at  $x = 8.0(mm)$ . The lower RPM however should result in lower energy and force values.

Figure 30 shows there is a difference between the measurements at  $x = 5.0(mm)$  and  $x = 8.0(mm)$  due to the second test of the knife operation at 27 RPM. The force difference (and its standard deviation) are 0.8% (2.2%) and 14.4% (5.9%) at  $x = 5.0(mm)$  and  $8.0(mm)$ . The energy difference (and its standard deviation) are 0.1% (3.4%) and 10.1% (6.3%) at  $x = 5.0(mm)$  and  $8.0(mm)$ . In this case the standard deviation increased when the indentation ( $x$ ) also increased. The results might be related to the knife test “RPM: 27 t1” because the stiffness graph displays an unexpected drop. After the unexpected drop the standard deviation for the two tests at 27 RPM rises from 0.1% at  $x = 5.0(mm)$  to 10% at  $x = 8.0(mm)$

A relationship between the RPM and the knife deterioration cannot be confirmed due to the measurement error. It can be concluded that two measurements per knife are not enough due to the possibility of measurement errors.

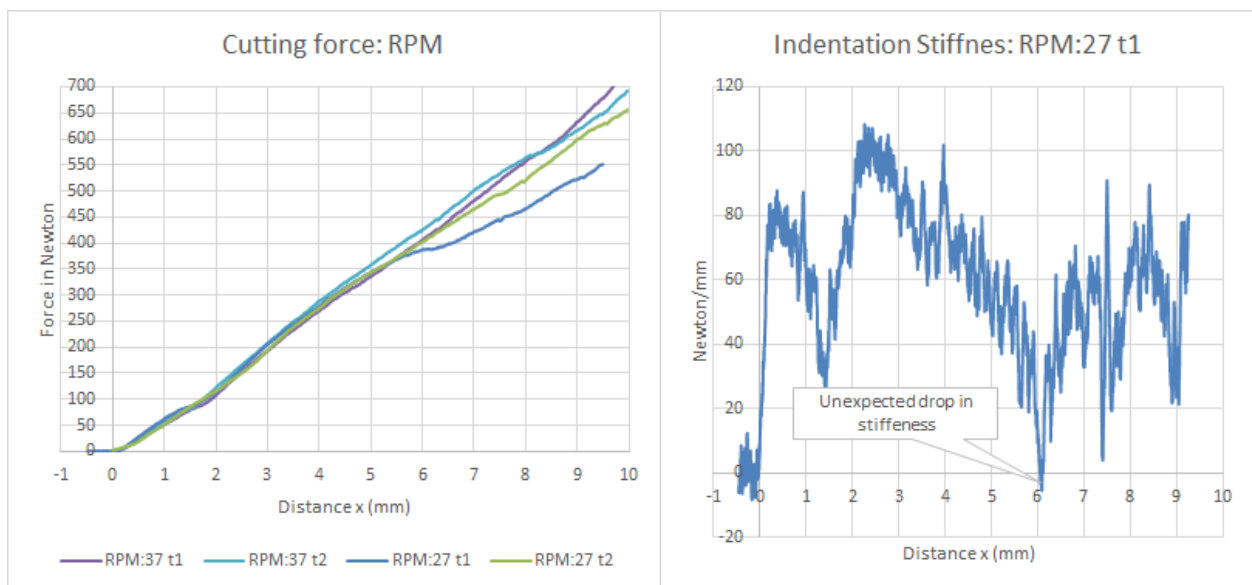


Figure 30: Comparing knives from two slicers that produced at 27 and 37 RPM. Right: the stiffness graph of a questionable sample.

## 4.5 RESEARCH QUESTIONS

The first research question reads:

*How to define a knife sharpness index for non-straight edge knives?*

Section 2.4.2 describes how the BSI is used to objectively measure straight-edge knives using Eq.1. Chapter 2 also explains that the BSI method is not directly applicable to non-straight edge knives. Therefore, different parameters that can influence the data collection required to verify the non-straight edge knives are verified in section 3.2. Section 4.1 proves that fracture toughness can be acquired from the measurements of the second wedge angle instead of a straight piece of knife as used for straight edge blades. An objective a knife sharpness index for non-straight edge knives was successfully defined and is unrelated to the substrate type or width.

The second research question reads:

*How can data of a knife analysis be used to develop a prediction model for knife sharpness deterioration?*

Section 4.2 confirmed that the BSI method cannot be applied to the non-straight edge knife sharpness test due to a high standard deviation. Section 4.4.1 until section 4.4.3 explain that the force and the total consumed energy observed during steady state cutting can be used to quantify the knife sharpness. The average of two tests per knife was used to create a general deterioration formula for the force and energy between 3 and 24 hours of production:  $F_{force} = F_{initial} \times (23.1\% + 1.5\% \times h)$  and  $E_{energy} = E_{initial} \times (16.4\% + 1.7\% \times h)$ . In section 4.4.3 it was found that two tests per knife are not enough due to measurement errors.

## 5 DISCUSSION AND CONCLUSION

Section 5.1 of this chapter contains the discussion of the results and include recommendations for further research. Section 5.2 addresses the limitations of the method and the chapter ends with the conclusion.

### 5.1 RESULT DISCUSSION

The BSI values in section 4.1 are inconsistent is due to the different values for cut initiation depth, energy and force. The observed differences are probably related to the geometry of the knives. A straight edge blade exerts force in the X and Y direction. Whereas the complex shape of a non-straight edge knife used at Vierverlaten exerts force in the X, Y and Z direction. A slight difference in the manner at which the knife comes into contact with the substrate changes the direction of the force in the X, Y and Z direction of a certain point. The change of forces in point Q also alter the forces in the X, Y and Z direction of the neighbouring points causing a chain reaction resulting in high volatile cut initiation parameters. This has not been proven and is also hard to simulate due to the fact that particles and forces shift in real time on a Nano scale in a three dimensional space. When  $x > 4.0(mm)$  and steady state cutting initiates, the knife settles around the geometry of the triangular shaped blade resulting in values that can be benchmarked.

The difference observed in sharpness of a new knife and a factory sharpened knife at  $x = 3.0(mm)$  and  $x = 8.0(mm)$  is related to the sharpening procedure. The fraiser in the knife production factory is set at the right distance to create a straight blade. The fraiser at Vierverlaten creates a frontal angle as displayed in Figure 31. The frontal angle corresponds to the findings from section 4.3 where factory sharpened knives require less force than a new knife to cut  $x = 3.0(mm)$  and more force to cut  $x = 8.0(mm)$ . These findings suggest the manner of sharpening also determines how well knives are able to penetrate substrates. The literature in section 2.3 proved that creating a lower first wedge angle increases the initial sharpness of the knives but also decreases the durability of the knife. Further research can be conducted to the shape of the knife. By creating knives with various wedge angles and analysing the cutting performance of the different knife wedge angles directly after the knives are sharpened and after a production run of 20 hours it can be determined how the wedge angle influences the cutting ability and the durability. Furthermore, other knife shape related properties such as the length of the first and second wedge angle can be analysed.



Figure 31: The left knife is sharpened at the factory and has a clear frontal angle. The right knife is new and has no frontal angle.

Knife deterioration between 3 and 24 hours of production is quantified according to the formulas:  $P_{force} = F_{initial} \times (23.1\% + 1.5\% \times h)$  and  $P_{energy} = E_{initial} \times (16.4\% + 1.7\% \times h)$ . the formulas are based on readings from five different points in time with a maximum duration of 24 hours. This limitation caused the function to be defined as a linear function while a test where knives are acquired with a shorter interval and longer duration can result in an exponential

deterioration function. A slicer has 24 knife blocks. Acquiring the first ten knives at an interval of one hour should provide enough information for a possible exponential deterioration trend. Acquiring knives at an interval of 3 hours for the remaining 14 knives result in a total duration of 52 hours. The knife sharpness regression model can be more accurately determined.

The unexpected observed increase in knife sharpness (section 4.4.1) after knives have produced beets for 20 hours requires further research. First of all because the standard deviation is higher than the observed difference with an unused knife. Secondly because the effect of the centrifugal force created by the cutting disk is unknown. And finally because used knives and unused factory sharpened knives have visual defects such as chipping and rough edges. Measurements should be conducted over the width of the knife. Thus from  $z = 0.0(mm)$  to  $z = 400.0(mm)$ .

Section 4.4.2 analysed the performance of different slicers. For this test only four of fifteen slicers were analysed. The slicers were chosen based on the location underneath the beet bunker and because multiple control room operators observed a difference in cossette quality for the selected slicers. These results point out that knife deterioration speed is not related to a single slicer and that the knife deterioration is equal. The observed difference in cossette quality can be related to the maintenance of the slicers. Most of the slicers date back to 1963 and have been incrementally upgraded with modern parts. The cutting disks for example are replaced once every five years. During the lifetime of the cutting disk the cutting blocks cause wear to the disk.

In the cutting test comparing the different slicers (section 4.4.2) it was found that knife deterioration is equal for all slicers and related to the total production time rather than their position underneath the beet bunker, it can be argued that the current method of choosing a slicer (to undergo a knife change) is incorrect. Knives are changed based upon the cossette quality as observed by the control room operator. Hereby the difference in cossette quality is not related to the sharpness of the knives but rather to the condition of the slicer itself. A repetition of this research on another row of slicers can confirm or invalidate this research.

No result was found for the relation between the RPM and the deterioration of knife sharpness in section 4.4.3 due to a measurement error in one of the two test runs. The results of successful test can be used to relate the slicer cossette production (in tons) to the knife deterioration. For further research it is recommended to perform three tests per knife.

## 5.2 LIMITATIONS

The discussed results have three noteworthy limitations:

The first limitation is the standard deviation. The initial resolution of 1:100 was based on the requirement to distinguish the knife sharpness between each 12 minutes of production. In the results the standard deviation for the observed force and energy fluctuates around 5%. The 5% difference translates to a resolution of 1:20. From the tests described in section 3.2 it can be concluded that different cutting speeds and substrate widths did not impact the standard deviation. Changing the substrate from potato's to a polymer did decrease the standard deviation. This suggests that another substrate has the possibility to lower the standard deviation. It must be noted that the standard deviation can also be related to the geometry of the non-straight edge blade as described in section 5.1.

The second limitation is the relation of the force and energy parameters to the actual quality of the cosettes. It is currently unknown how the force and energy parameters relate to the cosette quality. With cosette quality is meant the ability to diffuse sugar from the sugar water. Cost efficiently. Further research should focus on this relationship.

The third limitation is the maximum allowable indentation. The tests to quantify the input parameters (section 1.3.2) are performed with factory sharpened knives that have a maximum measurable indentation depth of  $x = 9.1(mm)$  (section 2.3). Section 4.4 prove that at higher indentation, differences between knives become more noticeable. New knives have an equal length and can be measured up to  $x = 20.0(mm)$ . Therefore it is recommended to use new knives for all tests and develop a new clamp to analyse the knives at higher indentation.

## 5.3 CONCLUSION

The objective of this research was to find out how a knife sharpness measurement could be created for the non-straight edge knives used at Viervelaten to quantify the input variables.

The development of the blade sharpness index for the non-straight-edge factory knives lead to the verification and settings of the indentation test. Analysing the results concluded the force and energy observed at an indentation of  $x = 8.0(mm)$  can be used to quantify the variables.



## REFERENCES

---

- Asadi, M. (2006). *Beet-Sugar Handbook*. New Jersey, United States: John Wiley And Sons Ltd
- Atkins, A. G. (2005). Toughness and cutting: a new way of simultaneously determining ductile fracture toughness and strength. *Engineering Fracture Mechanics*, 72(6), 849–860.
- Brown, T., James, S. J., & Purnell, G. L. (2005). Cutting forces in foods: experimental measurements. *Journal of Food Engineering*, 70(2), 165–170.
- Maitah, M., Řezbová, H., Smutka, L., & Tomšík, K. (2016). European Sugar Production and its Control in the World Market. *Sugar Tech*, 18(3), 236–241.
- Marks, R., & Black, D. (1985). Methodologies to produce and assess standardized trauma to the skin. *American Journal of Industrial Medicine*, 8(4-5), 491–498.
- Marsot, J., Claudon, L., & Jacqmin, M. (2007). Assessment of knife sharpness by means of a cutting force measuring system. *Applied Ergonomics*, 38(1), 83–89.
- McCarthy, C. T., Hussey, M., & Gilchrist, M. D. (2007a). On the sharpness of straight edge blades in cutting soft solids: Part I – indentation experiments. *Engineering Fracture Mechanics*, 74(14), 2205–2224.
- McCarthy, C. T., Ní Annaidh, A., & Gilchrist, M. D. (2010). On the sharpness of straight edge blades in cutting soft solids: Part II – Analysis of blade geometry. *Engineering Fracture Mechanics*, 77(3), 437–451.
- McGorry, R. W., Dowd, P. C., & Dempsey, P. G. (2005). A technique for field measurement of knife sharpness. *Applied Ergonomics*, 36(5), 635–640.
- O’Callaghan, P. T., Jones, M. D., James, D. S., Leadbeatter, S., Holt, C. A., & Nokes, L. D. (1999). Dynamics of stab wounds: force required for penetration of various cadaveric human tissues. *Forensic Science International*, 104(2-3), 173–178.
- Portela, S. I., & Cantwell, M. I. (2001A). Cutting Blade Sharpness Affects Appearance and Other Quality Attributes of Fresh-cut Cantaloupe Melon. *Journal of Food Science*, 66(9), 1265–1270.
- Portela, S. I., & Cantwell, M. I. (2001B). Cutting Blade Sharpness Affects Appearance and Other Quality Attributes of Fresh-cut Cantaloupe Melon. *Journal of Food Science*, 66(9), 1265–1270.
- Reilly, G. A., McCormack, B. A. O., & Taylor, D. (2004). Cutting sharpness measurement: a critical review. *Journal of Materials Processing Technology*, 153-154, 261–267.
- Saukko, P., & Knight, B. (2015). *Knight’s Forensic Pathology Fourth Edition*. CRC Press.
- Schuldt, S., Arnold, G., Kowalewski, J., Schneider, Y., & Rohm, H. (2016). Analysis of the sharpness of blades for food cutting. *Journal of Food Engineering*, 188, 13–20.
- Schuldt, S., Arnold, G., Roschy, J., Schneider, Y., & Rohm, H. (2013). Defined abrasion procedures for cutting blades and comparative mechanical and geometrical wear characterization. *Wear: An International Journal on the Science and Technology of Friction Lubrication and Wear*, 300(1-2), 38–43.
- Tsai, P. H., Lin, Y. Z., Li, J. B., Jian, S. R., Jang, J. S. C., Li, C., ... Huang, J. C. (2012). Sharpness

improvement of surgical blade by means of ZrCuAlAgSi metallic glass and metallic glass thin film coating. *Intermetallics*, 31, 127–131.

United States Department of Labor. Bureau of Labor Statistics. (2001). Current Population Survey, February 2000: Displaced Workers, Employee Tenure, and Occupational Mobility Supplement. *ICPSR Data Holdings*. <https://doi.org/10.3886/icpsr03169>

van der Poel, P. W., Schiweck, H. M., & Schwartz, T. K. (1998**part A**). *Sugar Technology: Beet and Cane Sugar Manufacture*.

van der Poel, P. W., Schiweck, H. M., & Schwartz, T. K. (1998**Part B**). *Sugar Technology: Beet and Cane Sugar Manufacture*.

Verhoeven, J. D., Pendray, A. H., & Clark, H. F. (2008). Wear tests of steel knife blades. *Wear: An International Journal on the Science and Technology of Friction Lubrication and Wear*, 265(7-8), 1093–1099.

Werner, R. A., & Franzblau, A. (2018). How can we best estimate the incidence and prevalence of carpal tunnel syndrome? *Muscle & Nerve*. <https://doi.org/10.1002/mus.26148>

Wieringa, R. J. (2014). *Design Science Methodology for Information Systems and Software Engineering*.

Zhou, D., & McMurray, G. (2009). Modelling of blade sharpness and compression cut of biomaterials. *Robotica*, 28(02), 311.



## APPENDIX A: BEET PRODUCTION

---

### ***A1 Beets & transport***

The beet harvester removes the green leaves and slices a slab from the top of the sugar beet root. This removed slab is the growing point of the sugar beet and contains high levels of impurities, which impede the factories ability to extract the sugar from the remainder of the harvested root.

The farmer is notified on the pickup date and temporarily stores the harvested beets on his property. 8000 businesses have a combined total of 15000 beet collection locations. Cosun has thirty-five cranes traveling through the Netherlands that load the beets into trucks. 15 of those cranes load beets for Viervelaten and truck carrying 30 tons arrives each three minutes at (with the exception of Sunday from 8:00 to 16:00. The result of fifteen loading location is a constant mix of beets. However there are multiple types of beets and some beet types have to be harvested earlier than others. Clay beets for example, due to the rain later on in the season they have to be harvested earlier. This is one of multiple causes that do cause seasonal similarities in supply.

### ***A2 Reception***

At reception the truck with the beets is weighed and a sample is taken. After delivery the empty truck is weighed again to determine the exact weight of the load in kg. The sample is used to verify the quality of the beets and the information is stored in a database. Data from the sample contains the terra (sand and mud) content, the sugar content of the beets, K-, Na- and other contents that reduce the recoverability of sugar. Farmers get paid based on the weight and the information of the sample (e.g. sugar content).

The trucks delivers the beets at the pre factory storage. A shovel driver slightly mixes the beets delivered minimize variation of the beet input of the factory. Since the beets constantly arrive from eight different locations throughout the country a mix is already ensured. Finally the shovel driver loads the mix onto a conveyor belt that transports the beets to the washing area.

### ***A3 Washing***

Four drum washing machines are used to clean the beets from terra stones and other field debris. Terra causes wear and tear in the production line. Acceptable is 0.2% terra content of the dry weight of a beet. The first drum removes the terra using water in counter current. The second drum is used to remove stones by using their high density. The third drum removes weeds, wood, loaf and other unwanted greens. The last washer is an after washer to further lower the terra content using water. Water exiting the washing station is called terra water and its sugar content is 0.4-0.6%. Terra water is pumped to settling fields, the terra settles on the bottom of the fields and the water is filtered and reused. The unwanted greens are filtered and transported to the pulp press to continue as dry pulp. Stones are collected and sold.

due to the rotational cutting disk (Figure 5) varies from 5.04 (km/h) at 20 RPM on the left side of the knife block to 25 km/h at 60 RPM at the right side of the knife Higher RPM increases the throughput and

### ***A4 Slicing of the beet***

A conveyer transports the beets from the washing department to the beet bunker. Underneath the beet bunker are three rows with five slicing machines. Appendix B shows the slicer layout underneath the beet bunker. The bunker is filled with approximately one meter to spare. This minimizes falling damage to the beet and ensures constant pressure on the beets that are fed into

the slicers. Each row of slicers is connected to a brewing trough. The position of the beet slicer underneath the bunker determines its pressure and the level of contamination. Contaminations e.g. terra and debris tend to crawl towards the middle of the beet bunker while the rounder beets roll to the outer edges of the beet bunker. Slicers located on the edges (e.g. slicer 10, 13) experience less knife deterioration

Figure 32 displays a side and top view of the slicer. The red area of the side view displays the beet flow through the slicer. The top view of the slicer displays the contact area of the beets with the cutting disk. Stones and other larger debris automatically exit through the stone removal hatch. When this happens the slicer stops and the machine operator manually has to check the knives, close the hatch and restart the slicer.

During each shift a machine operator replaces the knives of six slicers. A slicer is chosen based on the quality of the cossettes it produces and the general lead time of the knives in a slicer is 20 hours. The slicer downtime related to a knife change is 15 minutes. Each slicer has a cutting disk with two sets of 24 knife blocks (Figure 5). While one set is in the machine, the machine operator prepares the other set for the next knife replacement. Two 20 cm knives are put into each knife block creating a knife width of 400mm. During production the speed of the rotational cutting disk (Figure 5) varies from  $4.92 \frac{km}{h}$  at 20 RPM to  $23.77 \frac{km}{h}$  at 60 RPM. To compensate for knife sharpness deterioration during production, the RPM of the knives increases to maintain the target throughput.

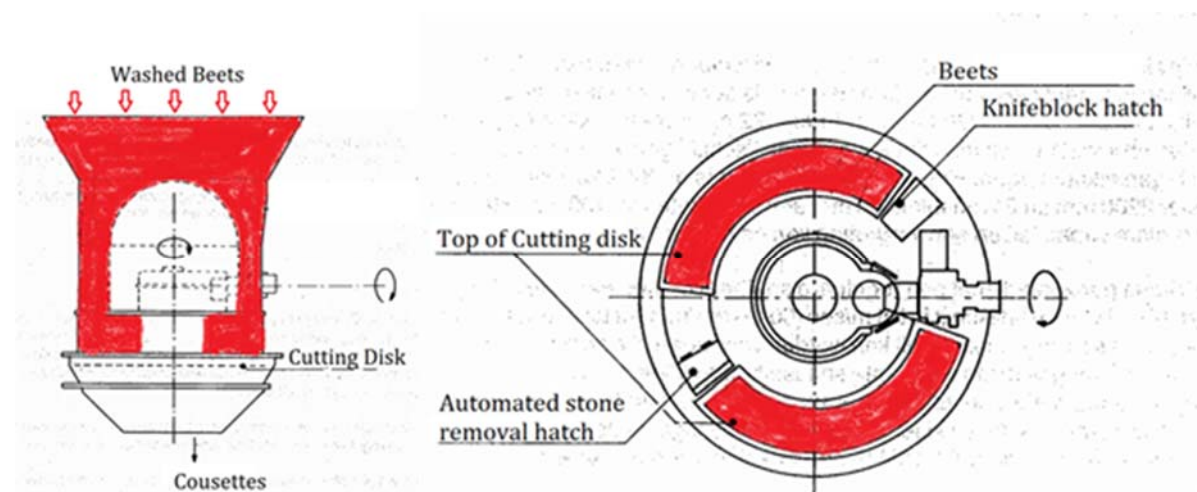


Figure 32: Cross-sectional side and top view drawing of a beet slicer at Viervelaten. The red parts indicate the location of the sugar beets during operation. Washed beets enter the slicer at the top and flow towards the top surface of the cutting disk. The cutting disk changes the beets into cossettes.

Increasing the surface area of the beets increases the diffusion of sugar. Therefore Type A and type B knives alternate each other to create V shaped cossettes (Figure 7) and maximize the surface area. The production of all the slicers in a row is measured in ton/hour and the RPM of all the slicers in a row is adjusted to achieve a set capacity point (Figure 33). If one slicer in the row stops, the rest will rev up to compensate.

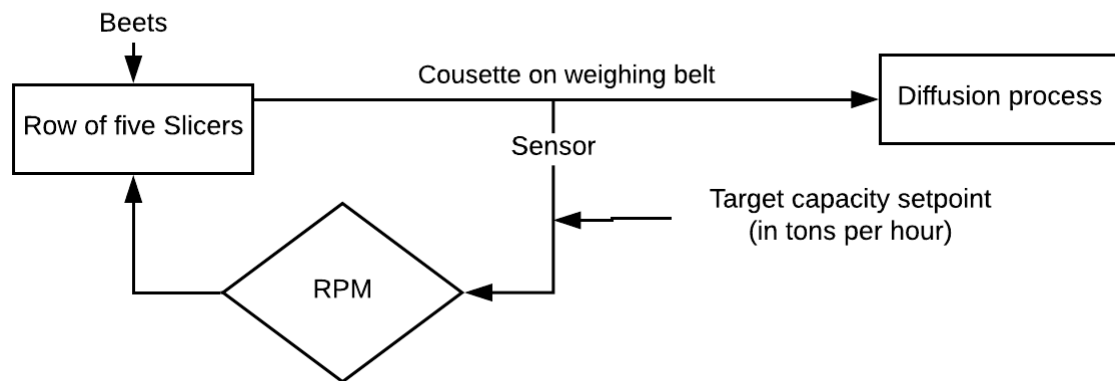


Figure 33: A flow diagram of the control system which ensures a predetermined target capacity is maintained.

As can be seen in Figure 34 a distance to the counter blade (a) is set to 7mm on all slicers and is continues for the whole campaign. The height (h) is set between 3.5 and 5.5 mm. changing the height is a tedious task and is done less than 3 times per campaign per slicer. Smaller distance for both parameters creates finer cossettes with a larger surface area but also a higher probability for mush (Appendix A5).

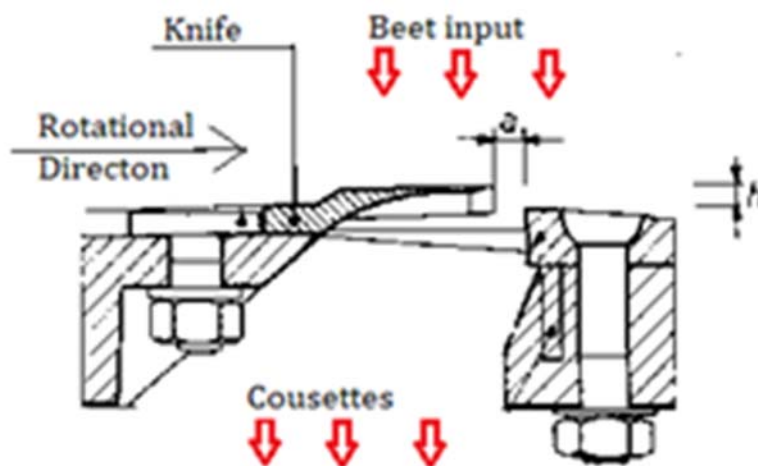


Figure 34: Cross-sectional side view drawing of a knife used at Volverlaten installed in a knife block.

### A5 Juice production

Diffusion into water is used to extract the sugar from the cossettes. A factory layout of the juice production is provided in appendix B2. The cossettes enters the brewing trough together with juice from the diffusion tower. In twenty minutes the temperature will rise to 70 degrees and the mixture will be viscous enough to be pumped to the bottom of the diffusion tower. Vanes in the diffusion tower steer the mixture up and it exits at the top of the diffusion tower 90 minutes later as wet pulp. The wet pulp is pressed to extract the water and feed it back into the top of the diffusion tower. Press Water and fresh water enters at the top of the diffusion tower and flows in opposite direction to ensure maximum sugar diffusion. The juice (sugar water) is extracted at the bottom of the diffusion tower through a filter and looped back to the brewing trough. After water has been looped back 3 to 4 times from the brewing trough to the diffusion tower it exits the system from the brewing trough and it is now called thin juice. Appendix B2 contains a snapshot of the process flows during operation.

Mush particles are cossettes smaller than one centimetre in length and cause filter of the diffusion tower to become clogged. Mush is created if:

- The cossette quality entering the brewing trough is low.
- The temperature in the juice production cycle is over 73 degrees Celsius, pectin is starting to break down as shown in Figure 35. Pectine provides the structure of the cells.
- Ph is too high or too low. Ph impacts cell wall breakdown. 5-8-6.0 is ideal

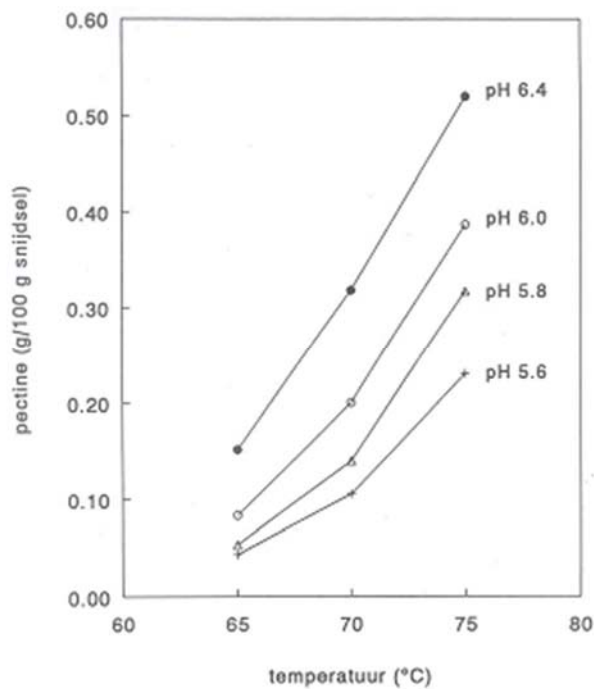


Figure 35: Graph displaying the breakdown of Pectin for increased temperature and/or increased pH. This negatively influence the strength of the cossettes. Dutch translation (van der Poel, Schiweck, & Schwartz, 1998b)

The first problem related to high mush content is the aforementioned filter clogging. This has to be solved by lowering the juice extraction until the mush has cleared from the filters. This takes around 10 to 20 minutes.

The second problem is that the duration of smaller particles in the diffusion tower is equal to the small mush particles. The combined mush particles have a higher surface area and will therefore diffuse other particles in the water such as egg whites and Pectine. (van der Poel et al., 1998b)

#### **A6 Purification of the juice**

The raw juice has to be purified for optimal crystallization since contaminated water has a higher boiling point. Part of the non-sugars particles in the raw juice are precipitated by mixing the raw juice with hot milk of lime. In the next step carbon dioxide is bubbled through the solution precipitating the lime as calcium carbonate (chalk). The chalk particles entrap and absorb non sugar particles. The chalk particles are separated from the juice by filters. The juice exiting the purification step is called thin juice.

### ***A7 Juice concentration***

The juice is separated from the water in two steps, juice concentration and juice crystallization. By first concentrating the thin juice to thick juice the load on the crystallization plant is significantly reduced. The overproduction of thick juice is also stored during the beet campaign and fed back into the crystallization plant after the beet campaign has ended.

The thin juice is converted into thick juice by boiling the water via multiple-effect evaporation. Thin juice enters the first column, each step the pressure is lowered thus decreasing the boiling point of water.

In a multiple-effect evaporator, water is boiled in a sequence of vessels. For multiple-effect evaporator to work only the first vessel has to be heated, after which the next vessel is held at a lower pressure than the last causing the boiling temperature of water to decrease. SuikerUnie Ververlaten recently upgraded to a seven stage evaporator after which thick juice has a Brix index of 72. A brix index indicates a dry-substance content measured by refractometer, expressed as mass percentage.

### ***A8 Crystallization and centrifugation***

Thick juice is fed to the crystallizers and refined sugar is added. Crystals can more easily attach to the crystals from the added refined sugar. Large vacuum cookers are used to further increase the sugar content and crystallization. The crystallization process is monitored continuously to guarantee optimal crystal growth. Using centrifuges and the aforementioned cooker, sugar at Ververlaten is produced in three stages. A, B and D stage. The first produced sugar is called A-sugar. The syrup residue is used in the next cooking stage to create B-sugar and syrup. The B-syrup is used to create D-sugar and massecuite, French for “Cooked mass”.

## APPENDIX B

### B1 LAYOUT OF THE SLICERS UNDERNEATH THE BEET BUNKER.

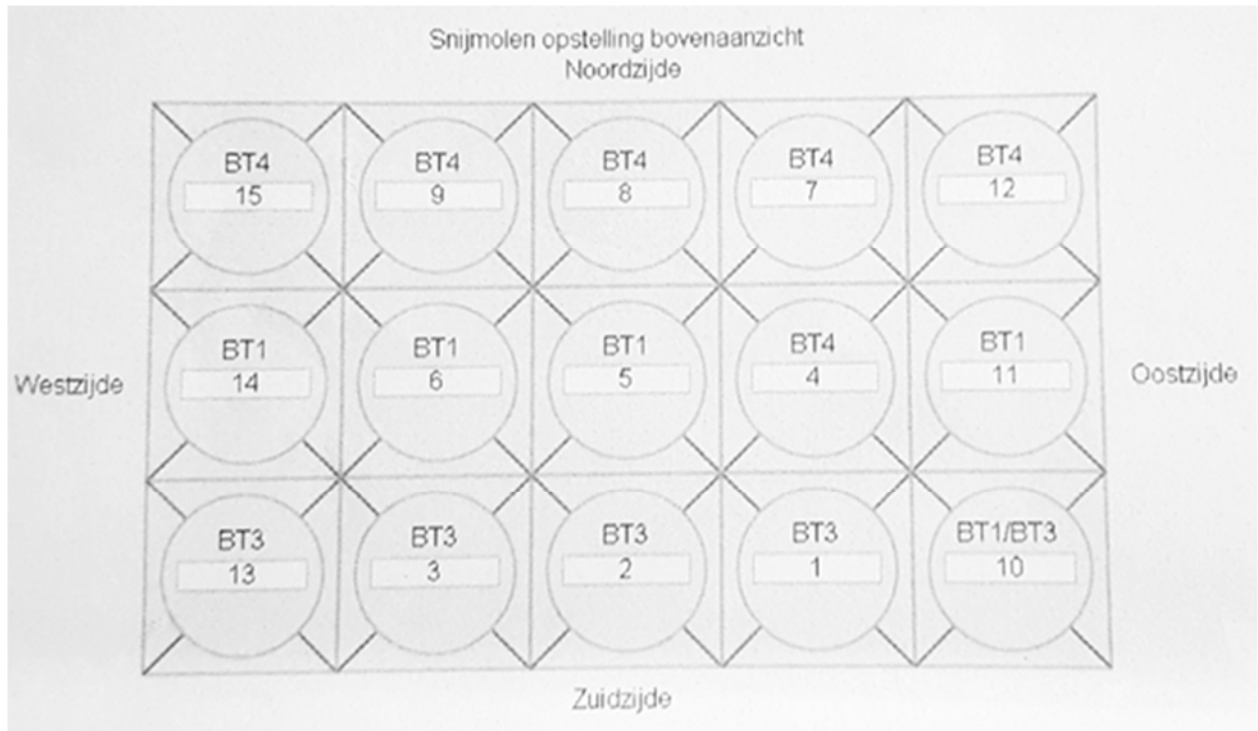


Figure 36: A top view of the slicer layout underneath the beet bunker. Each row is connected to a different brewing trough (BT). Slicer 10 can either be connected to BT1 or BT3. Furthermore, the row from slicer 15 is connected to BT4 and the row from slicer 14 is connected to BT1. Each BT is connected to a Diffusion tower. So TB4 is connected to diffusion tower 4. However, due to incremental factory expansions and flexibility an extra diffusion tower (DT3) is used. DT3 is connected to BT4 and BT1. The bottom row of slicers is only connected to BT1 and DT1.

## B2 SCHEMATIC AND DETAILED LAYOUT OF THE JUICE PRODUCTION

